BOTULINUM TOXIN TYPE A SPREAD INTO NON-INJECTED ANTAGONISTIC MUSCLES CAUSES INCREASED EXTRACELLULAR MATRIX COLLAGEN

by

İsmail Orkun Akcan

B.S., Bioengineering, Yıldız Technical University, 2013

Submitted to the Institute of Biomedical Engineering
in partial fulfillment of the requirements
for the degree of
Master of Science
in
Biomedical Engineering

Boğaziçi University
2019

ACKNOWLEDGMENTS

First and foremost, I would like to express my gratitude to my thesis advisor, Prof. Dr. Can A. Yücesoy, for introducing me to such an illuminating field of science and for his guidance throughout my study. Furthermore, I would like to thank my thesis examining committee Assist. Prof. Duygu Ege and Prof. Dr. Sevil Özgül Yücel for their valuable comments and recommendations.

I would like to thank my fellow friends in Biomechanics Laboratory Filiz Ateş, Ahu Nur Türkoğlu, Agâh Karakuzu, Cemre Su Kaya and Uluç Pamuk for their support and advice. I would also like to thank my friends in Biomedical Engineering Institute Bige Vardar and Sevgi Öztürk for being there.

Just as importantly, I would like to acknowledge the existence of individuals that I relate to as my chosen family and feel blessed to get to have them in my life at such a phase, Bilgen Coşkun, Cem Özvarlık, Aziş Özvarlık, Erdal Özvarlık, Can Özvarlık, Didem Özkaya, Deniz Bektaş, Büşra Parlak, Kemal Nalbantoğlu, Mine Kostak, Fatoş Dönmez, Seda Gani, Gülşah Köksalanlar, Mustafa Atilla Akgül, Filiz İnanoğlu, Geerte Piening, Oğuz Yenilmez, İrem Karakılınç, Gamze Demirtaş Taşçı, Mustafa Taşçı, Erinç Ermin, Beril Ermin and Kübra Sarıdağ.

Finally, I would like to dedicate this dissertation to my mother, followed by my sister, father, grandmother and two cats, Massimo and Trish. Everything is possible thanks to their unconditional love, endless patience, priceless support, relentless encouragement and unique chivalry. Together we grow stronger, together we prosper.

This study is granted by the project "Comprehensive Experimental Assessment of Previously Unknown Effects of Botulinum Toxin on Muscle Function". Principal investigator (TUBITAK Research Fund, grant no: 116S393).

ACADEMIC ETHICS AND INTEGRITY STATEMENT

I, İsmail Orkun Akcan, hereby certify that I am aware of the Academic Ethics and Integrity Policy issued by the Council of Higher Education (YÖK) and I fully acknowledge all the consequences due to its violation by plagiarism or any other way.

Name :

Signature:

Date:

ABSTRACT

BOTULINUM TOXIN TYPE A SPREAD INTO NON-INJECTED ANTAGONISTIC MUSCLES CAUSES INCREASED EXTRACELLULAR MATRIX COLLAGEN

The present study aims at assessing effects of Botulinum toxin type A (BTX-A) on the targeted medial and lateral gastrocnemius muscles in terms of muscle forces and connective tissue content. The particular goal is to test if BTX-A spreads from the injected muscles into the antagonistic anterior crural muscles and to test if those non-injected muscles have collagen wise denser extracellular matrix. For this purpose, an experimental animal study was conducted in the rat lower leg by measuring muscle forces and the density of collagen using histology. In order to assess the effects of BTX-A two cases were studied: BTX-A group and control group. Active force production, passive resistance, joint range of motion and connective tissue contents of these cases were compared. Muscle length-force relationships showed active force drops (up to 80%) and narrowing of length range of force exertion for target muscles (by 3 mm). However, also the antagonistic muscles showed force drops (around 20%) indicating inter-antagonistic leakage of BTX-A. In addition, the collagen density increased by 50% and 31% for target muscles, 11% for synergistic muscles, and 43% and 28% for antagonistic muscles. A major finding obtained from histological assessments is denser collagen results in a net increase at extracellular matrix of muscles whether they are targeted by BTX-A injection or not. It is evident that this effect arises from the spread of toxin. Such effect has important clinical implications.

Keywords: Botulinum Toxin, Experimental Animal Study, Histology, Collagen, Extracellular Matrix.

ÖZET

BOTULİNUM TOKSİN TİP A'NIN ENJEKTE EDİLMEMİŞ ANTAGONİSTİK KASLARA SIZMASI EKSTRASELLÜLER MATRİKS KOLAJEN MİKTARINI ARTIRMAKTADIR

Gerçekleştirilen çalışmada Botulinum toksin tip A etkilerinin hedef kaslar olan medial ve lateral gastrocnemius kaslarında, kas kuvvetleri ve bağ doku içeriği kapsamında incelenmesi hedeflenmiştir. Toksinin enjekte edildiği kaslardan antagonistik anterior crural kaslarına sızıp sızmayacağı ve eğer sızarsa toksin ile direkt enjekte edilmemiş bu kasların kolajen bazında daha yoğun ekstrasellüler matrikse sahip olup olmayacaklarının test edilmesi özellikle amaçlanmıştır. Bu amaçla sıçan alt ekstremitesinde kasların kuvvet üretimini ölçen ve kolajen yoğunluğunu histolojik metodlarla çözümleyen bir deneysel hayvan çalışması gerçekleştirilmiştir. Botulinum toksin etkilerininin incelenmesi için iki durum oluşturulmuştur: Deneysel grup ve kontrol grubu. Bu grupların aktif kuvvet üretimleri, pasif dirençleri, eklem hareket açıklıkları ve bağ doku içerikleri karşılaştırılmıştır. Kas uzunluk-kuvvet ilişkileri hedef kaslarda %80'e kadar aktif kuvvet düşüşü ile birlikte 3 mm civarı kuvvet ortaya konulan uzunluk aralığında daralma göstermiştir. Bununla birlikte antagonistik kaslarda da gözlenen %20 civarı aktif kuvvet düşüşü toksinin inter-antagonistik sızdığına işaret etmiştir. Aynı zamanda, kolajen yoğunlu hedef kaslar için %50 ve %31, sinerjist kaslar için %11 ve antagonistik kaslar için %43 ve %28 artmıştır. Histolojik değerlendirmelerden açığa çıkan önem teşkil eden bir sonuç ise kolajen miktarındaki yükselişin kasların ekstrasellüler matrikslerinde net bir artışa, enjeksiyona direkt maruz kalıp kalmamalarına bakmaksızın sebep vermesidir. Bu etkiye hedef kastan antagonist kasa sızan toksinin neden olduğu aşikardır. Bu tür bir belirti ise önemli klinik çıkarımların açık bir göstergesidir.

Anahtar Sözcükler: Botulinum Toksin, Deneysel Hayvan Çalışması, Histoloji, Kolajen, Ekstrasellüler Matriks.

TABLE OF CONTENTS

LIST OF FIGURES

LIST OF TABLES

LIST OF SYMBOLS

μ	Micro sign
$\pm$	Plus-minus sign
m	Meter sign
g	Gram sign
mg	Milligram sign
kg	Kilogram sign
$^\circ$	Degree sign
Δ	Greek Capital Letter Delta
%	Percentage sign
’	Modifier Letter Apostrophe
α	Greek Small Letter Alpha
e	Logarithm, Euler’s Number
N	Newton sign
P	P value at statistics
®	Registered sign
+	Plus sign
−	Minus sign
σ	Standard Deviation
U	Atomic Mass Unit
h	Hour sign
ml	Milliliter sign
F_p	Muscle Passive Isometric Forces
F_a	Active Muscle Forces
ms	Millisecond sign
th	Greek letter theta, Θ
mA	Milliampere sign
Hz	Hertz sign, frequency

LIST OF ABBREVIATIONS

PCSA	Physiologic Cross-Sectional Area
ACh	Acetylcholine
MTJ	Myotendinous Junction
BTX-A	Botulinum Toxin type A
BTX	Botulinum Toxin
SD	Standard Deviation
GM	Gastrocnemius Medialis
GL	Gastrocnemius Lateralis
TA	Tibialis Anterior
EDL	Extensor Digitorum Longus
SOL	Soleus
FT	Force Transducer
ANOVA	Analysis of Variance
LM	Light Microscopy
EM	Electron Microscopy
VAC	Vacuum Assisted Closure
TES	Tissue Embedding Station
ROI	Region of Interest
RGB	Red Green Blue
K-S	Kolmogorov-Smirnov
CNTRL	Control group
EMFT	Epimuscular Myofascial Force Transmission
CP	Cerebral Palsy
ECM	Extracellular Matrix
EHL	Extensor Hallucis Longus

1. INTRODUCTION

1.1 Skeletal Muscle

1.1.1 Structure

Skeletal muscle fibers are like body cells that have highly specialized functioning to produce force and movement. A muscle cell also named as a myocyte [1] is the type of cell found in muscle tissue. Myocytes go through a process called myogenesis [2] to form muscles and the striated cells of cardiac and skeletal muscles that they form are referred to as muscle fibers [1],[3]. Endomysium is the deepest and smallest component of muscle connective tissue and it encases every single muscle fiber. Collagen is the major protein which composes connective tissues like endomysium. Endomysium has been shown to contain chiefly type I and type III collagen components and subsidiary type IV and type V [4]. Connective tissue is continuous and present in all muscles as fascia. Surrounding each muscle is a layer of connective tissue known as the epimysium; encircling each fascicle is a layer called the perimysium and enveloping each muscle fiber is a layer of connective tissue called the endomysium. Altogether they combine the skeletal muscle extracellular matrix (ECM). The various layers of the extracellular matrix, forming the endomysium, perimysium and epimysium of skeletal muscles, provide essential structural, biochemical and mechanical support to contractile fibers. Muscle cells are cylindrical with a diameter ranging from about 10 to about 100 μm. A muscle fiber's diameter determines its force production, and alterations of fiber diameters in mature muscles indicate a change at the level of muscle use. Fiber length has a subtle impact on fiber contraction velocity and the distance over which the fiber can shorten. Endomysium surrounds the muscle fiber with its structure composed of collagenous tissue in a form of mesh-like sheath.

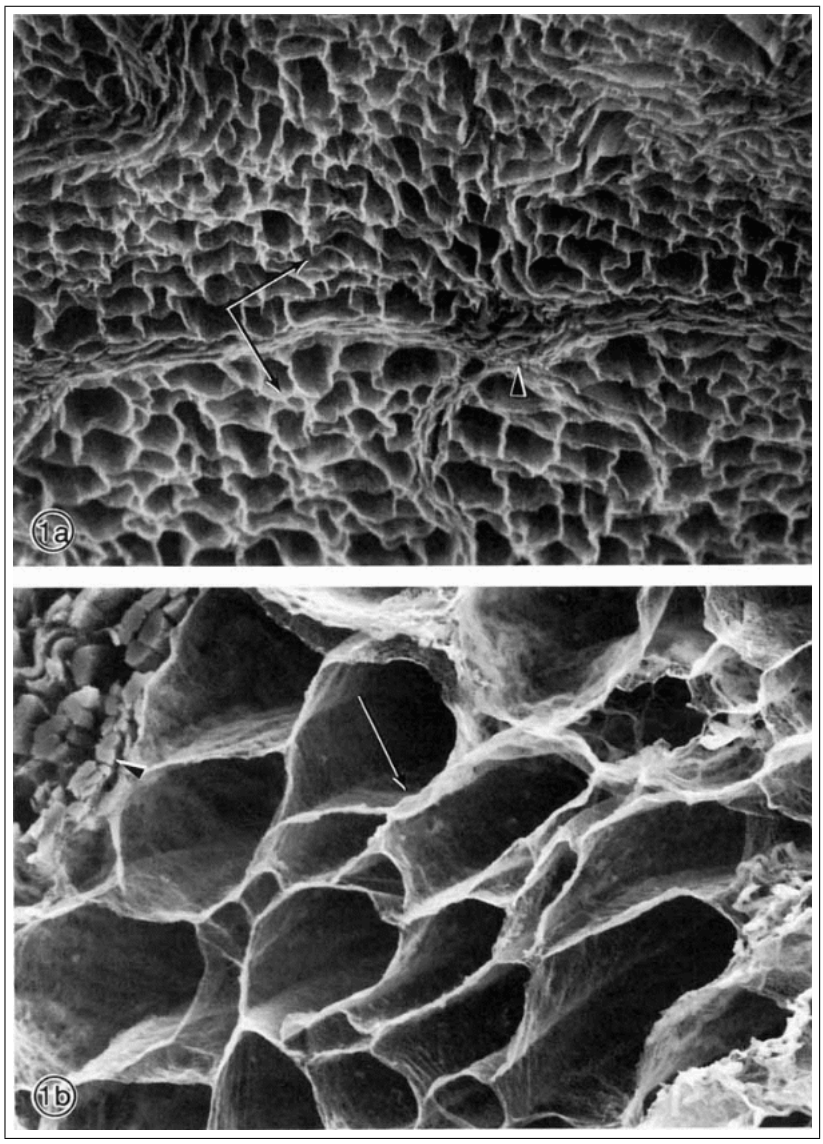

Figure 1.1 Scanning electron micrograph of the endomysial connective tissue within skeletal muscle. This image was generated by removing muscle fibers through acid digestion. (1a) View with lower magnification of connective tissue in which the arrowhead points to perimysial connective tissue while the arrows point to individual endomysial tubes. (1b) View with higher magnification in which the arrowhead points to undigested muscle fibers while arrow points to a single endomysial plane [49].

Perimysium surrounds the muscle fascicles formed of muscle fibers each surrounded by endomysial tissue. Epimysium surrounds the muscles composed of bundles of fascicles. Muscle cells have contractile filaments throughout their structures. Sarcomeres arranged in series forms a string called myofibril, which is the largest functional unit of contractile filaments and they are arranged in parallel to make up the muscle fiber. Muscle fiber length and diameter determines the number of sarcomeres within a fiber which essentially determines the function of muscle fiber. Series arrangement of

sarcomeres in myofibril allows the myofibrillar shortening to sum up to the total distance of shortening distances of all the individual sarcomeres. Hence, a whole muscle may shorten up to several centimeters even though a sarcomere can only shorten about 1 μm.

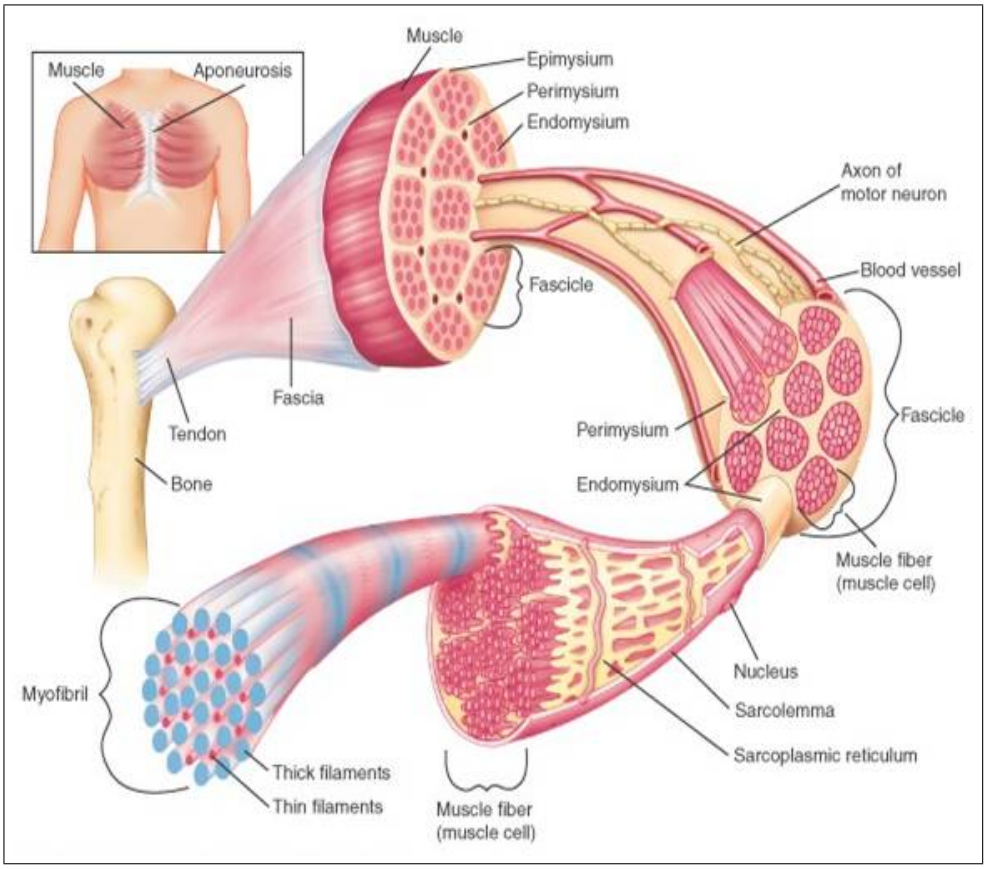

Figure 1.2 Structural hierarchy of skeletal muscle. Note that the connective tissue coverings, the epimysium, perimysium, and endomysium, are continuous with each other and with the tendon. Note also that muscle fibers are held together by the perimysium in groups called fascicles. Muscle fibers are composed of myofibrils arranged in parallel. Myofibrils are composed of sarcomeres arranged in series. Sarcomeres are composed of interdigitating actin (thin) and myosin (thick) filaments [48].

Myofilaments are contractile filaments that compose sarcomeres. Contractile filaments are divided into two sets: thick filaments and thin filaments. They are the representative of large polymers of the myosin and actin proteins. The myosin-containing filaments, called thick filaments, and the actin-containing filaments, called thin filaments, form a hexagonal lattice and this pattern gives muscle its striped appearance allowing it to shorten through the active interdigitation of these filaments. Striated muscle is an alternative term to skeletal muscle due to this repetitive dark and light banding pattern under the light microscope. Sarcomere regions are named after

their appearances to establish references addressed to them. A-band defines the myosin filaments in the sarcomere region; I-band defines the actin filaments in the sarcomere region; H-zone defines the part of A-band in which there is no actin-myosin overlap; Z-band defines the dark narrow line which intersects I-band; and M-band defines the zone at the center of A-band. The distance from one Z-band to the next one defines the sarcomere length which is an essential determinant of force generation. The actin-containing filament regulates tension generation and the myosin-containing filament generates tension during muscle contraction.

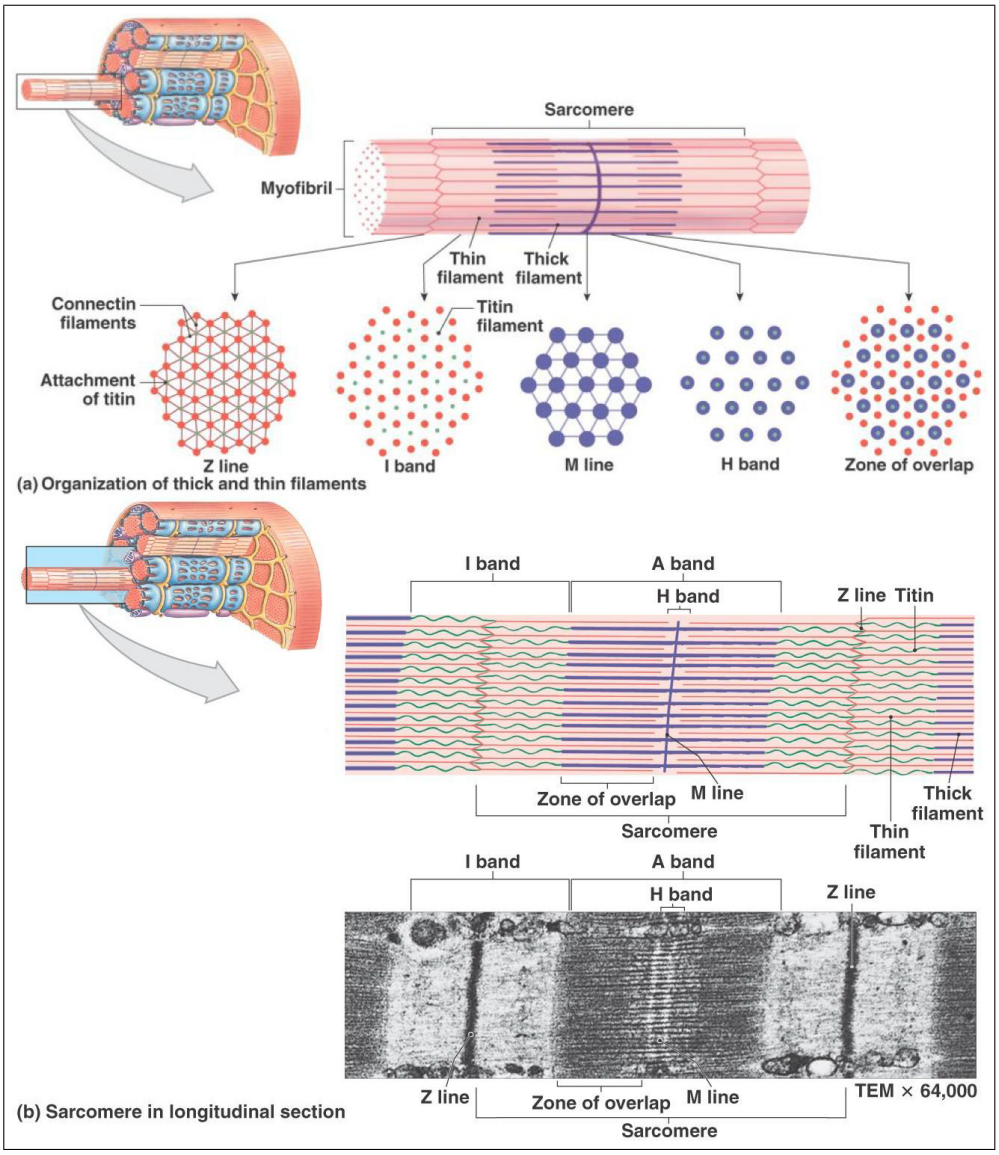

Figure 1.3 Schematic array of thick and thin filaments within sarcomere. (a) Hexagonal arrangement of interdigitating myosin and actin filaments that constitute sarcomere. (b) Representation of continuous form of sarcomere arrangement in paralleled series with an image of light microscopy demonstrating dark and light banding pattern of sarcomere [50].

Skeletal muscles attach to bones via connective tissue structures known as tendons and anatomically each muscle has an origin and insertion. Muscles often cross more than one joint and therefore exert an influence at multiple locations. Skeletal muscle architecture can be referred as "the arrangement of muscle fibers relative to the axis of force generation". Generally common types of fiber architectures are longitudinal, pennate and multipennate. Muscle architecture can be summarized with calculation of various parameters after measuring muscle mass, fiber length, sarcomere length, muscle length and pennation angle. These parameters directly affect the whole muscle's contractile properties and enables the calculation of so called physiologic cross-sectional area (PCSA) which is directly related to muscle's maximum tetanic tension. PCSA represents the sum of the cross-sectional areas of all the muscle fibers within the muscle and is essential to make valid estimations in human studies.

1.1.2 Skeletal Muscle Physiology

Muscle activation is the initial concept of skeletal muscle physiology and it begins with muscle contraction through neural activation. Excitation-contraction coupling is the precise process in muscle contraction in which neural activation occurs. Even though numerous microscopic sequences take place in this mechanism, acetylcholine (ACh) release plays a major part in it and aligned with the point of view of this study, it will be briefly introduced. ACh which is a neurotransmitter causing muscle fiber excitation, is stored at the end of the peripheral nerves. ACh is synthesized by motor nerves and transported down the axon to those ends. Nerve activation causes ACh to be released into synaptic clefts and through diffusion ACh binds to its receptor called ACh receptor. ACh binding triggers depolarization of muscle fiber sarcolemma and action potential emanates in all directions from the neuromuscular junction. Numerous enzymes take active roles in this mechanism and in order to study "spastic" like muscles, Botulinum toxin (BTX) is introduced into muscles which simply blocks neuromuscular transmission by intercepting the ACh release mechanism.

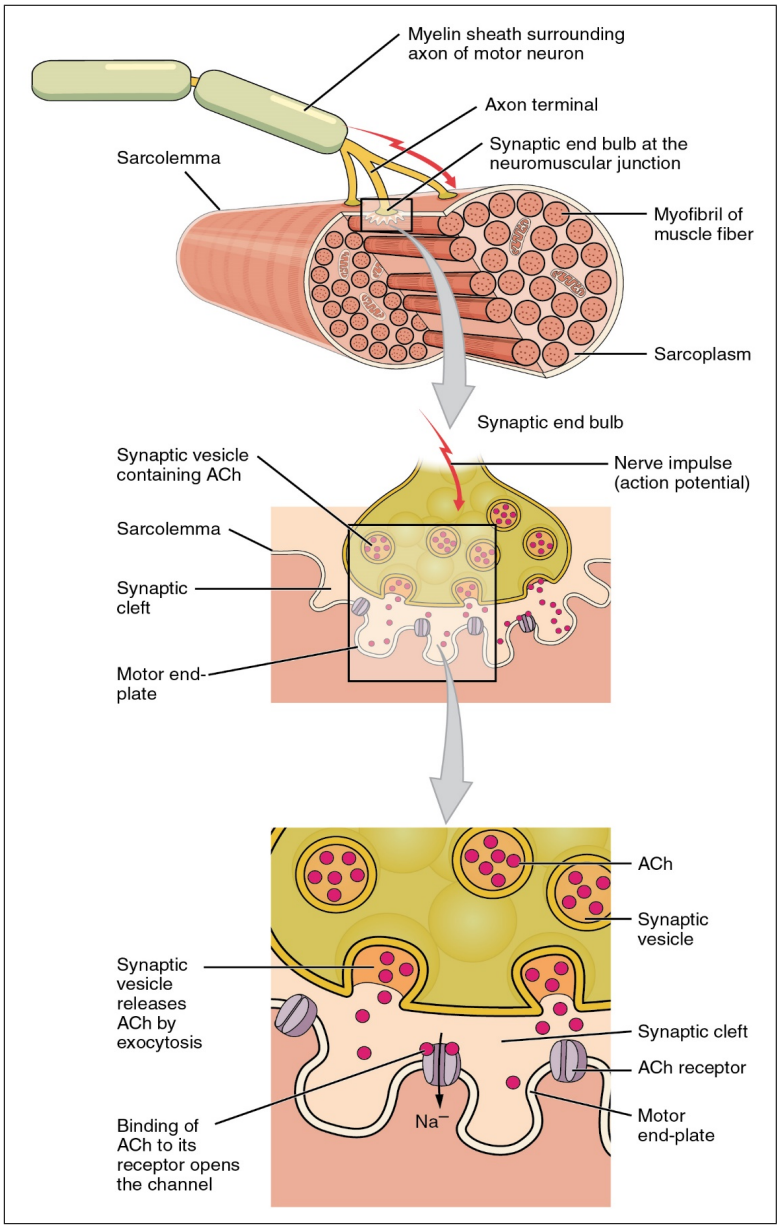

Figure 1.4 Representation of ACh release into synaptic cleft which is essentially required for muscle excitation. Following events occur in order: (i) generation of the peripheral nerve action potential; (ii) release of ACh from the presynaptic nerve terminal; (iii) binding of ACh to the muscle fiber ACh receptor on the postsynaptic membrane [48].

1.2 Force Transmission Pathways

Muscle fibers within sarcomeres generate muscle force. In order to achieve movement of body parts, force generated within sarcomeres must be exerted outside muscle fibers. Two fundamental approaches of force transmission are direct mechanics and in-

verse mechanics way. The direct way considers force being transmitted from sarcomeres to skeleton through tendons and the inverse way considers various additional subjects like reaction forces and how they are exerted. Both approaches should provide with the same answers and since inverse mechanics approach presents with more details, it will be the choice of interest. There are two kinds of compounds arranged in series with sarcomeres, tendons and fascia, distinguishing two different force transmission pathways.

1.2.1 Myotendinous Force Transmission

The myotendinous force transmission is suggested to be the primary pathway of force transmission within the muscle belly. Muscular connective tissues are in continuum together and they merge to form myotendinous junction (MTJ) and aponeurosis. Each muscle fiber is attached with an MTJ and myofibers significantly decrease in diameter at this end, with presence of collagen fibers at site it results in increased force per cross-sectional area per fiber. Force is assumed to be transmitted by these structures and if this is the one primary force transmission pathway, all forces of sarcomeres in series should be equal and sarcomere lengths within the myofiber should be identical as well. However, muscle is not an isolated entity and it interacts with various structures within body.

1.2.2 Myofascial Force Transmission

Additional to myotendinous sites, muscle fibers, fascicles and whole active muscles merge together through trans-sarcolemmal molecules, cytoskeletal lattice, basal lamina, and connective tissue hence all these compounds are connected to one another and in continuum together. Myofascial force transmission suggests that force is not exclusively transmitted to origin or insertion of muscle fibers but also onto endomysium and further onto intramuscular connective tissue stroma. This continuous matrix forms another level of force transmission mechanics and change mechanical equilibri-

ums of entire limb. Depending on their contributions to this mechanism of structures, myofascial force transmission can be divided into two categories:

1.2.2.1 Intramuscular Myofascial Force Transmission

Force generated by sarcomeres are transmitted through trans-sarcolemmal proteins via endomysium, epimysium and perimysium in order and ensures the continuity of transmission. Endomysial tubes packs myofibers and it forms a muscular connective tissue like a honeycomb which reaches to fascicle borders. Perimysium wraps fascicles in a similar way and reaches to epimysium which surrounds the whole muscle. Force transmission in this hierarchical intramuscular domain is named intramuscular myofascial force transmission.

1.2.2.2 Epimuscular Myofascial Force Transmission

Myofascial loads exerted onto muscle can be transmitted through epimysium onto intramuscular stroma. Directly connected collagenous connections on epimysium between synergist muscles provide with continuous form of myofascia which enables force transmission between them. Therefore, such transmission is defined as epimuscular myofascial force transmission (EMFT). This specific type of force transmission pathway is further called as intermuscular myofascial force transmission and particularly defines the transmission between synergistic muscles, exclusively.

Additionally, myofascial force transmission occurs between a muscle and extramuscular structures like blood vessels, nerves, fascia and collagenous tissues. This type of force transmission pathway is called extramuscular myofascial force transmission.

Structures mentioned above are compounds of a continuous fascial system and this makes it possible for variable force transmissions. EMFT has important effects such as proximo-distal force differences and unequal sarcomere lengths within muscles.

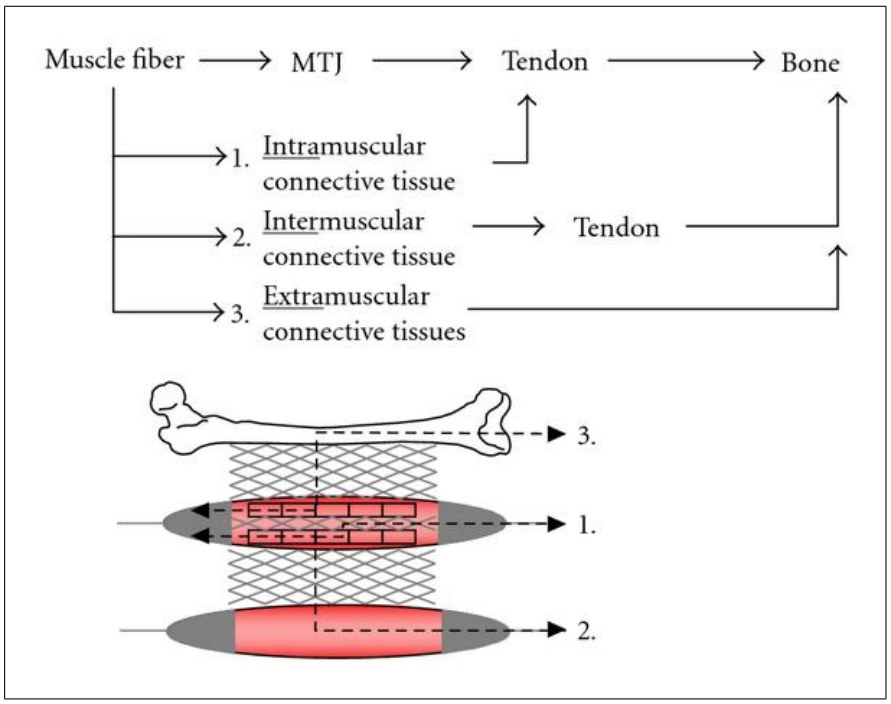

Figure 1.5 Schematic representation of the different pathways via which force generated within muscle fibers can leave the muscle to be transmitted to the skeleton. (1) Intramuscular pathway: force transmission occurs via cytoskeleton of fiber. (2) Intermuscular pathway: force transmission occurs between two neighboring muscles via the continuous connective tissue at their muscle belly interface. (3) Extramuscular pathway: force transmission occurs between a muscle and adjacent non-muscular structures. The term epimuscular myofascial force transmission is used to indicate transmission via inter- or extramuscular pathways [51].

Unequal forces are exerted at origin and insertion of muscle due to additional myofascial loads [5]. Force equal to additional load acts upon to force exerted at opposite end of muscle and net myofascial load causes sarcomeres to have longer lengths than other locations within same muscle fibers due to different active forces being exerted locally. Naturally, tendinous tissues are intact to myofascial connections that enables active forces of many muscles to act upon the insertion of another muscle [6],[7].

Extramuscular myofascial force transmission is emphasized to play a more important role than intermuscular transmission via dissection experiments [8]. Such pathway is the only theoretically possible way between antagonistic muscles' transmission since they are compartmentally separated. Neurovascular tracts and other fascial structures form stiff connections between antagonist compartments. Effects of such interaction are like those for synergistic muscles [9],[10],[11],[12].

1.3 Botulinum Toxin Treatment

Spasticity, a velocity-dependent resistance to stretch, occurs secondary to upper motor neuron lesions such as stroke, spinal cord injury and cerebral palsy (CP). Spasticity is clinically affiliated with stiffness, increased muscle tone, exaggerated stretch reflexes and joint contractures. Skeletal muscle of individuals with spasticity undergoes alterations at its structure and functionality such as decreased range of motion, decreased voluntary strength and increased joint stiffness. Contractures are extreme effects of mechanical resistance which can be prevented by early treatment of hypertonia with BTX in spastic CP. Accordingly, BTX-A is widely used in treating patients with CP. Toxin causes paralytic effect by blockade of neuromuscular transmission. Injection of it into a muscle causes chemodenervation and local paralysis. This effect is reversible hence the main factor of toxin being developed as a versatile therapeutic tool. BTX-A produces its paralytic effect by inhibiting the release of ACh from the presynaptic nerve terminal at neuromuscular junction which causes local chemodenervation. Partial muscle paralysis facilitates blocking the hyper-excitable stretch reflexes and decreases active force production. Reduced spasticity and decreased muscle tone are main aspects of BTX-A treatment. Consequently, the treatment is expected to improve function by acting in favor of agonist-antagonist force balance and increasing joint range of motion, while decreasing passive resistance of muscle at joint.

BTX-A is so far the most potent biological toxin known to humankind, hence there are apprehensible concerns regarding its use for therapeutic applications [13]. Majority of adverse effects of BTX originate from weakness of the muscles injected or those nearby, which become weak through regional spread of the toxin [14].

Improvements of function and movement expected to BTX-A treatment highly revolves around agonist-antagonist force imbalance of target muscles. Major expectations to improve function are increased joint range of motion and decreased passive resistance. However, recent animal studies conducted at rat lower extremity, precisely at anterior crural compartment, manifested that BTX-A application can decrease muscle length range of force exertion and increase muscle passive forces [15],[16]. These

reports are not aligned with the desired outcomes of BTX-A treatments but also contradict them. Furthermore, spread of toxin away from the injection site and targeted muscle is also reported for non-injected neighbouring muscle [17] and into all muscles of same compartment [18]. Those effects, which negate the treatment goals require further and detailed investigations. It is essential to study potential leak of toxin into an antagonistic muscle compartment.

1.4 Goal of the Study

The present study aims at assessing effects of BTX-A on the targeted medial and lateral gastrocnemius muscles both in terms of active and passive muscle forces and length range of force exertion, as well as their connective tissue content. The goal of the present study was to test the following hypotheses in a rat model: BTX-A injected into GM and GL; (1) decreases active forces of the antagonistic TA and EDL; (2) reduces length range of force exertion; (3) increases passive forces of TA and EDL; and (4) increases intramuscular connective tissue content.

2. METHODS

2.1 Animal Models

Surgical and experimental procedures were approved by the committee on the ethics of animal experimentation at Boğaziçi University. Male Wistar rats were divided into 2 groups: control (n=6; mean ± SD: body mass = 301.0 ± 26.9 g) and BTX (n=6; mean ± SD: body mass = 271.8 ± 33.3 g).

After imposing a mild sedation with an intraperitoneal dose of 1 mg/kg ketamine, entire lower extremity was shaved and calf muscle on lower hind limb was exposed. The gastrocnemius medialis (GM) and the gastrocnemius lateralis (GL) muscles were located by palpation when the ankle was in maximal dorsal flexion and the knee angle approximately 180° at prone position. Along the tendon, a marker was placed at a point 12 mm proximal to the musculo-tendinous junction on the GM. A second marker was placed 9 mm lateral to the first one on the GL. All injections were made exclusively into the gastrocnemius muscle of the left leg at two sites, medial and lateral heads, to a depth of 3 mm. The thickness of gastrocnemius muscle approximates 3.9 mm in plantar flexed positions [19] and the skin thickness approximates 0.7-1 mm. Based on this, the needles were marked 3 mm from the tip to ensure that the injections made at the marker locations remain within the target muscle.

For the BTX group, each 100-unit vial of vacuum dried, botulinum type A neurotoxin complex (BOTOX; Allergan Pharmaceuticals, Westport, Ireland) was reconstituted with normal saline solution. The animals received a double intramuscular BTX-A injection (one injection to medial head and another one at lateral head) at a total dose of 0.2 unit, 0.1 unit per each muscle head. The volume injected was 40 μl at total, 20 μl per each muscle head. The control group was injected with the same volume of normal saline solution exclusively. The dose selected was based on [20], which study tested the effects of a wide range of doses of BTX-A (from 0.02 U to 20.0 U) after a

single mid-belly injection to the tibialis anterior (TA) muscle of the rat. This showed even the smallest dose caused approximately a fifth of the total cross-sectional area to be paralyzed only 24 h following the injection. Presently we used an intermediate dose of 0.1 U for the GM and GL with comparable size to the TA.

The aim was to assess the short-term effects of BTX-A and all injections were performed 5 days prior to testing and dissection for histology work. It has been reported [21] that the greatest force decreases of rat lower hind limb flexors occur in the first 4 days after injection, which level off by day 5. On the other hand, nerve sprouting occurs after the first week [22]. Therefore, the time from BTX-A injections is suitable for testing after force decreases reach a steady state and before remodeling of the neuromuscular junctions take place. The animals were kept separately until the day of experiment in standard cages and in a thermally regulated animal care room with a 12-h dark-light cycle.

2.2 Surgical Procedures

The animals were anesthetized using intraperitoneally injected urethane (1.2 ml of 12.5% urethane solution per 100 g body mass). Additional doses were given if necessary (maximum 0.5 ml). Immediately after the experiments, the animals were euthanized with an overdose of urethane solution.

During surgery and data collection, the animals were kept on a heating a pad (Homeothermic Blanket Control Unit; Harvard Apparatus, Holliston, Massachusetts) to prevent hypothermia. A feedback system utilizing an integrated rectal thermometer allowed control of body temperature at 37°C by adjusting the temperature of the heating pad.

The skin and the biceps femoris muscle of the left hindlimb were removed, the calf muscles and the anterior crural compartment, including the extensor digitorum longus (EDL) and TA muscles, were exposed along with the triceps surae muscle group.

Only a limited distal fasciotomy was performed to remove the retinaculae (i.e., the transverse crural ligament and the crural cruciate ligament). The connective tissues of the muscle bellies within the anterior crural compartment and triceps surae muscle group were left intact. The tendon of the plantaris muscle was cut and the distal tendons of the gastrocnemius muscles were separated from the soleus (SOL) tendon as distally as possible and cut.

The combination of knee joint and ankle angles (120° and 100°, respectively) was selected as the reference position. In the reference position, the 4 distal tendons of the EDL muscle were tied together using silk thread. Matching markers were placed on the distal tendons of the EDL, TA, SOL and gastrocnemius muscles, as well as at a fixed location on the lower leg. Subsequently, the distal EDL tendon complex and the TA tendons were cut as distally as possible. The Achilles tendon was removed with a piece of bone from the calcaneus. The distal tendon of the SOL was dissected from the tendon complex.

The femoral compartment was opened for 2 purposes: (1) to reach the proximal tendon of the EDL – after reaching it, the tendon was cut from the femur with a small piece of the lateral femoral condyle still attached; and (2) to expose the sciatic nerve. After this was done, the sciatic nerve was dissected free of other tissues, and all nerve branches to the muscles of the femoral compartment were cut. Subsequently, the sciatic nerve was cut as proximally as possible.

To provide connection to the force transducers (FT), Kevlar threads were sutured to: (1) the proximal tendon of the EDL muscle; (2) the tied distal tendons of the EDL muscle; (3) the distal tendon of the TA muscle; (4) the distal tendon of the SOL muscle; (5) and the distal tendons of the gastrocnemius muscles.

2.3 Experimental Set-Up

The animal was mounted in the experimental set-up shown in Figure 2.1: The femur and foot were fixed with metal clamps with the ankle in maximum plantarflexion (180°) to allow for free passage of the Kevlar threads to the distal FTs. The knee angle was set at 120°. Each Kevlar thread was connected to a separate FT (FT; BLH Electronics, Inc., Canton, Massachusetts). Care was taken to ensure that the alignment of the Kevlar threads was in the muscle line of pull. The distal end of the sciatic nerve was placed on a bipolar silver electrode (Figure 2.1).

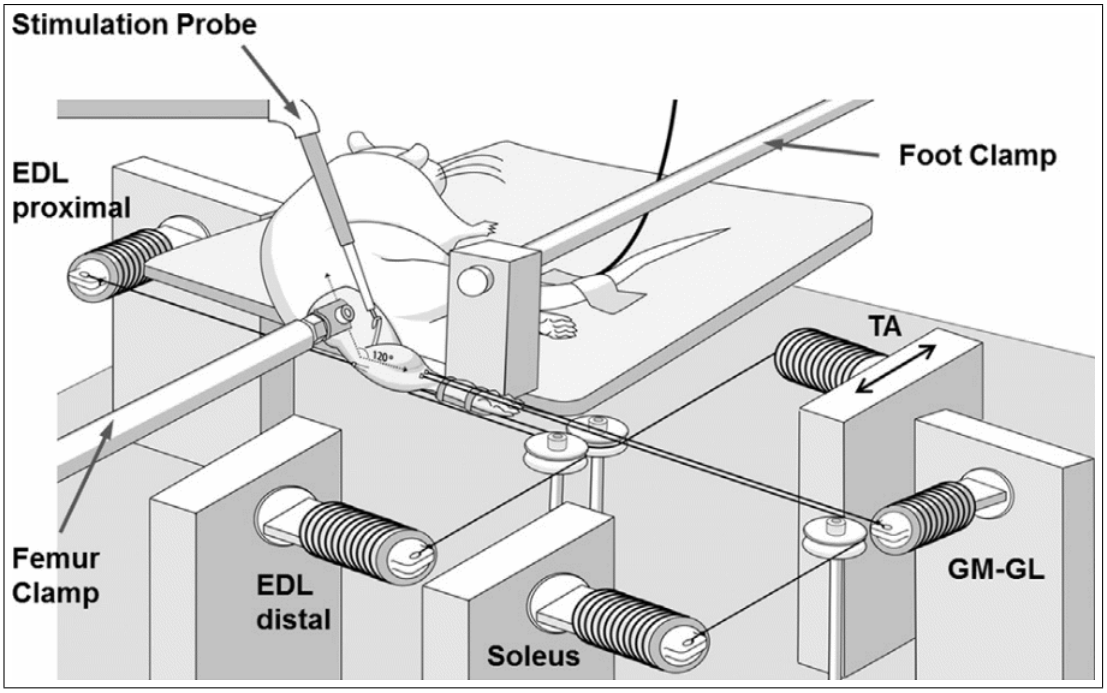

Figure 2.1 Schematic view of the experimental setup. (a) The tied distal tendons of the gastrocnemius medialis and lateralis (GM-GL), the distal tendons of soleus, tibialis anterior (TA), and extensor digitorum longus (EDL) muscles as well as the proximal tendon of EDL were each connected to a separate force transducer by Kevlar threads. The femur and the foot were fixed by metal clamps when the knee angle is 120° and the ankle angle is at maximal plantar flexion. The distal end of the sciatic nerve was placed on a bipolar silver electrode [52].

2.4 Experimental Conditions and Procedure

Room temperature was kept at 26°C. For the duration of the experiment, muscles and tendons were irrigated regularly by isotonic saline to prevent dehydration. Before acquiring data, GM-GL, SOL, TA and EDL muscle-tendon complexes and their connective tissues were preconditioned by isometric contractions, alternatingly at long and short GM-GL lengths, SOL lengths, TA lengths and EDL lengths until forces at short GM-GL, SOL, TA and EDL lengths were reproducible; effects of previous activity at long length [23] were removed. Experiments were performed in four conditions: (1) Only GM-GL muscle-tendon complex length was altered, whereas the SOL tendon was always kept in reference position, as well as anterior crural compartment muscles' tendons. (2) GM-GL and SOL muscle-tendon complex lengths were altered together, while anterior crural compartment muscles' tendons kept in reference position. (3) Only TA muscle-tendon complex length was altered, whereas the EDL tendons always kept in reference positions, as well as triceps surae muscle group muscles' tendons. (4) Both proximal and distal muscle-tendon complexes of EDL were altered together, whereas the TA tendon was always kept in reference position along with the triceps surae muscle group muscles' tendons.

The isometric forces of all calf muscles were measured simultaneously at various muscle-tendon complex lengths of the gastrocnemius, by moving its distal FT in the distal direction (i.e., distal lengthening condition). Starting from its active slack length, the gastrocnemius length was increased in increments of 1 mm until reaching 2 mm over the optimum length at conditions (1) and (2). The isometric TA force was measured at various muscle-tendon complex lengths. Starting at muscle active slack length, the TA length was increased by moving its FT in increments of 1 mm, until it was 2 mm over the length at which the highest TA force was measured at condition (3). EDL muscle position was changed first by moving its proximal and distal FTs by 5 mm proximally. From this proximal starting position ($\Delta\text{posit}_{\text{EDL}} = 0$ mm) on, the EDL position was manipulated by moving both of its FTs in 1-mm increments for a total of 5 mm in the distal direction until the end-distal position ($\Delta\text{posit}_{\text{EDL}} = 10$ mm). At each different EDL position, EDL and TA forces were measured simultaneously at condition (4).

Muscle passive isometric forces (Fp) were determined 100 ms after the second twitch in inactivated state. Muscle total isometric forces were determined during the tetanic plateau (the mean force for a 200 ms interval, 150 ms after tetanic stimulation). Data for active muscle force (Fa) calculated by subtracting the measured passive force from total force in relation to muscle-tendon complex length were fitted with a polynomial function using a least squares criterion:

$$y = b_0 + b_1 x + b_2 x^2 + \cdots + b_n x^n \tag{2.1}$$

Where y represents F_a, x represents muscle-tendon complex length. b_0 , b_1 , $\cdots$, b_n are coefficients determined in the fitting process. Data for passive muscle force in relation to muscle-tendon complex length were fitted with an exponential function using a least squares criterion:

$$y = e^{a_1 + a_2 x} \tag{2.2}$$

Where y represents F_p, x represents passive muscle-tendon complex length, and a_1 and a_2 are coefficients determined in the fitting process.

Polynomials that best described the experimental data were selected by using one-way analysis of variance (ANOVA). The lowest order of the polynomials that still added a significant improvement to the description of changes of muscle-tendon complex length and muscle force data were selected (minimally 4th and maximally 8th order polynomials were selected for the present data). Per muscle-tendon complex length, forces of each muscle were obtained by using these functions, averaged, and standard deviations (SD) were calculated to determine muscle force (mean ± SD).

Muscle optimal force (the maximum isometric force exerted by an active muscle) often is taken as an indication of a muscle's capacity for force production. The range from active slack length to length at which optimal force is exerted is taken as an indicator of movement capability with active force exertion within the potential range of motion of a certain joint. The polynomials obtained were also used to determine: the optimal force and active slack length of GM-GL, SOL and TA (condition I, II

and III). L_{range} was determined as the range between the active slack length and the length at which optimal force is measured. GM-GL and SOL muscle-tendon complex lengths expressed as deviation from GM-GL muscle-tendon complex optimum length (i.e., $\Delta l_{ma\_GM\text{-}GL}$). TA muscle-tendon complex lengths expressed as deviation from TA muscle-tendon complex optimum length (i.e., Δl_{ma_TA}).

All muscles studied were activated maximally by supramaximal stimulation of the sciatic nerve (STMISOC; Biopac Systems, Goleta, California, USA), using a constant current of 2 mA (square pulse width 0.1 ms). After setting the targets' muscle length, 2 twitches were evoked, and 300 ms after the second twitch the muscles were tetanized (pulse train 400 ms, frequency 100 Hz). At 200 ms after tetanic contraction, another twitch was evoked. After each application of this stimulation protocol, the muscles were allowed to recover for 2 minutes at reference position.

The TA, EDL, SOL, GM and GL muscles were removed immediately after the animal was euthanized and were prepared for histological assessment. The tissues were fixed and processed immediately using an automated tissue processor (TP1020; Leica Microsystems, Wetzlar, Germany) and embedded in paraffin (EG1150H; Leica). Five-micron sections were cut using a microtome (RM2255; Leica) for every 20 μm and stained with Gomori trichrome (30-30110; Bio-Optica Milan, Italy) which was used to distinguish intramuscular collagen [24],[25].

2.5 Tissue Fixation for Histological Assessment

In order to preserve tissues as "lifelike" as possible, biochemical and proteolytic processes being inactivated, and structures being immobilized and locked in space by a "fixation" step is crucial. Chemical and physical fixation methods are two main approaches that are normally used to "fix" biological samples. The most common approach is the chemical fixation by immersing the tissues into a fixative, which kills and stabilizes the cell contents used in specimen preservation for light microscopy (LM) and electron microscopy (EM). Fixing agents are traditionally classified as "coagulant"

or "non-coagulant" based on their effect on soluble proteins in solution. Fixation of proteins and protein complexes has two major mechanisms: denaturation, and addition and cross-link formation. Coagulant fixing agents such as ethanol and methanol can induce protein denaturation by removing and replacing free water in cells and tissues, resulting in conformation change of protein molecules and their solubility. Ethanol and methanol are usually combined with other fixing agent(s) as a fixative for light microscope. On the other hand, acetic acid is a non-coagulant fixing agent even though it coagulates nuclear proteins and assists stabilization and helps prevention of loss of nucleic acids. Acetic acid does not react with proteins and commonly used with ethanol as a cytological fixative because it counteracts the shrinkage effect of ethanol and preserves nucleic acid at the light microscope level. Carnoy's fluid (Absolute alcohol, 60 ml; Chloroform 30 ml; Glacial acetic acid, 10 ml – 6:3:1) has been suggested for histochemical studies of proteins [26] and glycogen [27] because it does not cause irreversible chemical changes in the reactive groups. Carnoy's fluid penetrates very rapidly and results in excellent nuclear fixation while preserving the nissil substance and glycogen smoothly. Therefore, Carnoy's fixation was the best choice of interest due to our target molecule glycogen. It is also a good choice of fixative for carbohydrates and causes considerable shrinkage and dissolves majority of the cytoplasmic elements.

The fixation process is affected by several factors such as buffering, penetration, volume, temperature, concentration and time interval. Alcohol penetrates fastest and penetration into a thick section will occur more slowly than for a thin section. The volume of fixative should be a 10:1 ratio of fixative to tissue and increasing the temperature, in a chemical fixation and as with all chemical reactions, will increase the speed of fixation. Concentration of fixative should be kept at the lowest level possible considering the expenses and time interval from tissue dissection to placing the tissue into the fixative is crucial. For this regard, the faster is the better.

Table 2.1
Fixation Procedure for EDL, TA, SOL, GM and GL.

Tissue	Fixative	Ratio	Duration
EDL	Carnoy's	10:1	2 hours
TA	Carnoy's	10:1	4 hours
SOL	Carnoy's	10:1	2 hours
GM	Carnoy's	10:1	4 hours
GL	Carnoy's	10:1	4 hours

2.6 Tissue Processing for Histological Assessment

The fixation was followed by tissue processing where the tissue is infiltrated with a suitable histological wax and embedded into, mostly paraffin, in order to get microscopic tissue sections via microtome. This process can be performed manually but to use an automated tissue processor is more efficient since they employ raised temperatures, effective fluid circulation and vacuum cycles that enhance processing. Tissue processing includes 3 main phases described as dehydration, clearing and infiltration. Wet fixed tissues require water to be removed from them because melted paraffin is hydrophobic and immiscible with water, so that dehydration takes place in a series of alcohol solutions of increasing concentration until pure, water-free alcohol is reached. Clearing is the subsequent step and even though the tissue is water-free at this state, alcohol, which replaced water is immiscible with melted paraffin. Therefore, a clearing agent that is miscible with both alcohol and melted paraffin is required. The most common clearing agent is xylene and it is usually followed by toluene and chloroform at practice. Finally, the third phase of tissue processing, infiltration, in which the tissue can now be infiltrated with paraffin.

Table 2.2
Tissue Processing Procedure for EDL, TA, SOL, GM and GL.

Substance	Duration
96% ethanol	20 minutes
100% ethanol	20 minutes
Xylene	20 minutes
Xylene	20 minutes
Paraffin (57° - 60°C) VAC	1 hour
Paraffin (57° - 60°C) VAC	2 hours

2.7 Tissue Embedding for Histological Assessment

Paraffin infiltrated tissue cassettes are placed at paraffin bath of Tissue Embedding Station (TES) and metal block molds are warmed up at storage area of TES. Paraffin infiltrated tissues are removed from the tissue cassettes and poured a little hot paraffin to the bottom surface of empty molds and placed tissues on top of them. Tissues are orientated by using heated forceps as desired and labeled empty tissue cassettes are placed on top of the molds and covered with hot paraffin. Molds are then shifted to the cold plate (-15°C) of Tissue Cooling Station. Processed tissues are now embedded in paraffin. Embedded tissues are kept in room temperature overnight before separation from the metal blocks in order to prevent cracks forming. The metal blocks are very briefly kept on the cold section. Extra care should be taken when embedding the tissues in order to actually obtain cross-sections and to avoid longitudinal sections.

2.8 Tissue Sectioning for Histological Assessment

Embedded tissues must be cut into sections via microtome in order to be placed on microscope slides. Microtome mechanism was set to 5 μm distance and FEATHER® A35 stainless steel microtome blades are used. Sectioning tissues is challenging and requires much skill and a lot of practice and owing to this special care is taken during sectioning to prevent tearing, folding, and ripping. Water bath was kept

very clean, when necessary, alcohol was added to the water bath to increase the surface tension, and paraffin sections were never kept longer than 30 seconds in the water bath, which provides just enough time to remove wrinkles. Afterwards they were picked up on a microscope slide and were labeled with pencil and left alone to dry. After drying they were taken to incubator for 12 hours at 37°C which enhances the section adhesion to the slides.

2.9 Tissue Staining for Histological Assessment

Paraffin containing tissues are not penetrable by any stains so far. Therefore, a rehydration step which is simply just the opposite of the dehydration step at tissue processing is essential before initiating the tissue staining. This rehydration step removes paraffin out of the tissues and allows water soluble dyes to penetrate the sections. This process begins with xylene (or a substitute of it) followed by a serious of alcohol of decreasing concentrations until pure water is reached and ends with it. Various dyes exist for their diverse abilities to stain differing cellular components of tissues. Hematoxylin and eosin are the routine stains and the rest of the stains are called as special stains and become a choice of interest according to the research or diagnostic needs. Trichrome stain contains chromotrope 2R, the plasma stain, and fast green FCF, the connective fiber stain, and has a specific use to demonstrate collagen and muscle in tissues or to differentiate collagen and muscle in tumors. In clinical pathology, it is used to identify increases in collagenous tissues or to indicate fibrotic changes. It is also used to distinguish tumors rooted from muscle cells and fibroblasts, yet it is the choice for distinguishing histological changes that occur in neuromuscular diseases. The principle usage for trichrome is to differentiate collagen from other eosinophilic structures, such as muscle fibers. Additional to staining, in order to preserve the specimen for several years after staining procedure is complete, a mounting media is required between the specimen and cover glass. Entellan is a water-free mounting medium which allows specimen to be permanently mounted for microscopy. Entellan contains toluene and it should be used with water-free specimens processed with xylene prior to mounting. Mounting media are viscous, clear liquids with superior light-refraction properties. The

anhydrous mounting media in their dissolved form can be easily and safely dropped without smearing via dropping bottles onto the stained and dehydrated specimen, and the slide can be covered airtight with a cover glass. The evaporation of the intermedium results in the form of a hardened, solid, clear film of mounting medium under the cover glass, preserving the stained specimen material. Thus, the sample can be observed under a microscope without any interference.

Table 2.3
Tissue Staining Procedure for EDL, TA, SOL, GM and GL.

Rehydration	
Substance	Duration
Xylene	10 minutes
Xylene	10 minutes
96% ethanol	2 minutes
96% ethanol	2 minutes
90% ethanol	2 minutes
80% ethanol	2 minutes
70% ethanol	2 minutes
Distilled water	2 minutes
Trichrome Staining	
Substance	Duration
Distilled water	8 minutes
Hematoxylin	1.5 minutes
Distilled water	15 seconds
Tap water	4 minutes
Distilled water	1 dip
Trichrome	15 to 40 minutes
0.2% acetic acid	10 seconds

2.10 Image Taking for Histological Assessment

Common LM methodology used for stained histological specimens is brightfield microscopy; unless the study does not need fluorescence imaging particularly. Light microscopes are used to perceive niceties and enlarged images of little entities. It is hard to see much element in live cells under the microscope, because cells inclined to be colorless and transparent. This motivates fixation and staining at histology work for cells to be imaged under LM.

The present study aimed to capture images of tissue sections of lower extremity muscles of rats stained with Gomori Trichrome so brightfield microscopy was ideal to gather the desired outcome in a highly enough, efficient and accurate way. Brightfield microscope has four components as Light Source, Condenser Lens, Objective Lens, and Eyepiece/Camera. Light source usually includes a halogen bulb as light source which illuminates sample below and delivers light through it to condenser and objective lenses. Condenser lens gathers light from source and focuses it to sample. Objective lens gathers light transmits through sample and intensifies details by a chosen factor of magnification. Eyepiece simply views and/or records images. LM sections require a certain thinness to transmit enough light that can reach to eye through specimen, objective lens and eyepiece in order so that the sections in study were cut at 5 μm. Glass slides were mounted on object stage with aperture to support them. Objective with magnifying power 4 was used to examine entire area of tissue sections and detect area of interest. Target areas were observed under objective with magnifying power 10. Images were taken via microscope imaging software called Leica Application Suite by setting certain parameters as given below, composing standardization for images all together.

Table 2.4
Light Microscope Settings for Image Taking.

Magnification	x10	Light	6
Exposure	1.68	Gain	3.3x
Saturation	0.80	Gamma	2.37

2.11 Image Processing for Histological Assessment

A color based semi-automated segmentation method was implemented. The first step of this process asked user to prescribe the collagenous regions by drawing a free-hand region of interest (ROI) on one of the histology images from the image stack, simply guiding user to make color sampling.

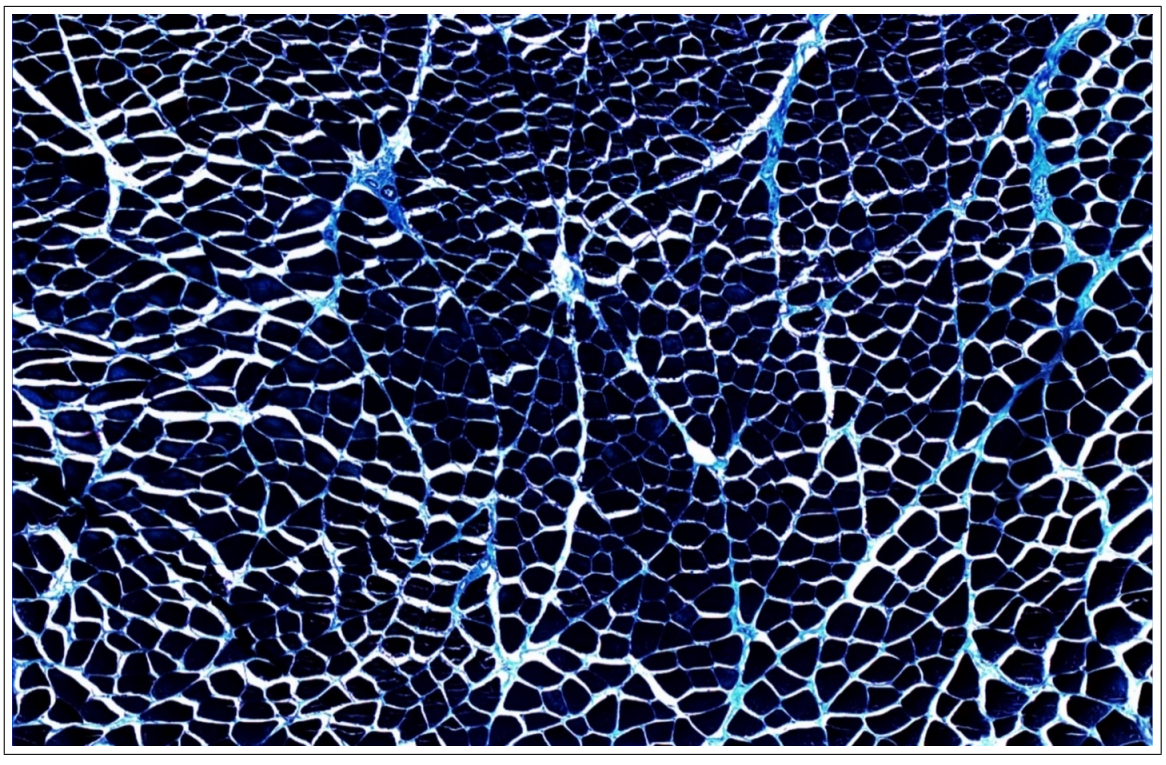

Figure 2.2 Sample histological section of tibialis anterior stained using Gomori trichrome. The section exemplifies intramuscular tissue content for BTX-A group with 10x magnification. Gomori trichrome stain gives a light (green to blue) color to the connective tissues.

The image was then masked by this user-specified ROI and transformed from RGB to CIE-LAB color space to compute deltaE units, which is a commonly preferred metric for measuring color difference between a reference and a target pixel [28],[29],[30]. In this case, computing the color difference between the pixels of connective tissue region and rest of the pixels at the image in deltaE units was done. In the present study, mean color values of the pixels falling inside of the ROI was considered as the reference color, and deltaE values were quantified for the remaining pixels in the image. Next, the calculated deltaE image was displayed to the user for interactive threshold determination which can be named as tolerance threshold. To select a proper threshold, the user was allowed to move a cursor on the displayed image and to update the threshold value. Segmented image was displayed for each update until the user regarded segmentation as successful.

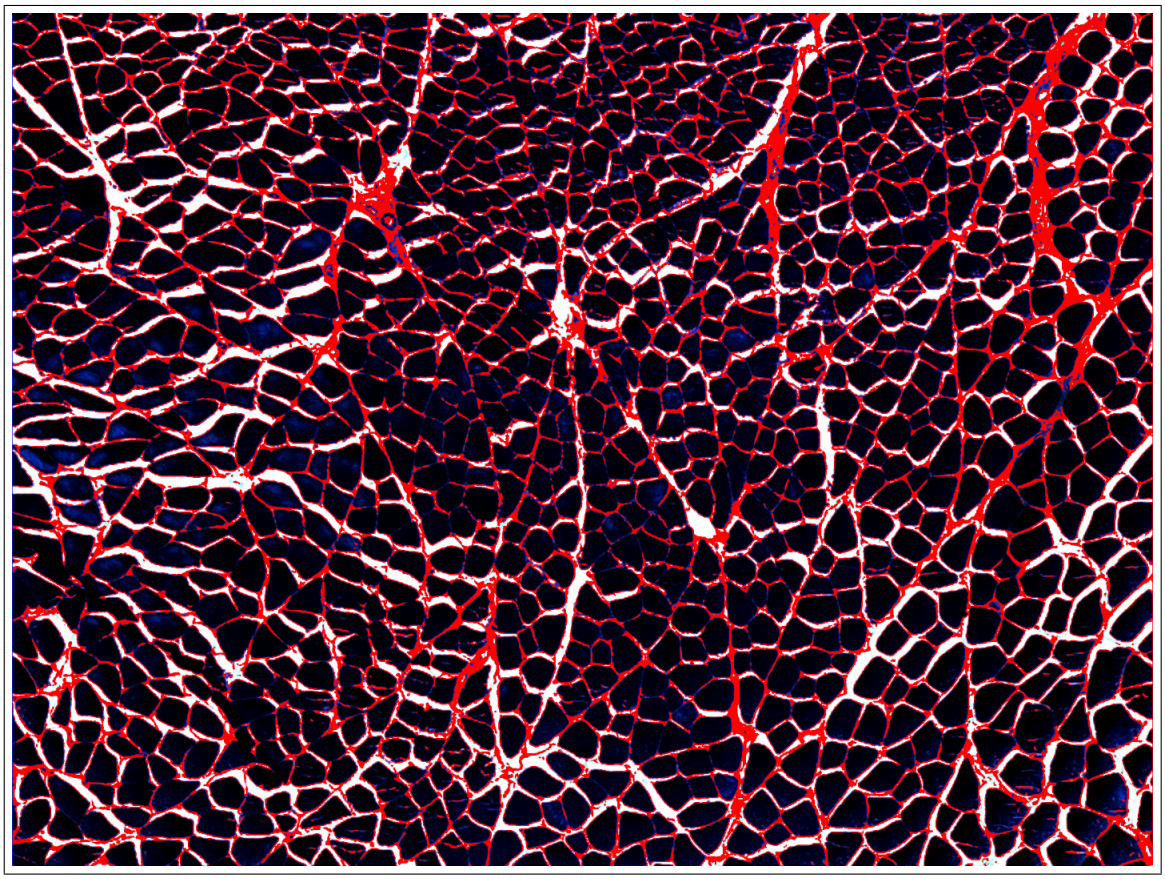

Figure 2.3 Sample histological section of tibialis anterior stained using Gomori trichrome at previous figure processed by user specific code to differentiate collagenous structures. Muscle fibers' pixels remain same where collagenous structures' pixels get marked with red color for further analysis.

The remaining images from the stack were automatically segmented using the parameters obtained for the first image. After segmentation of collagenous region, edge detection was performed using Prewitt operator to localize pixels that define the contour of regions such as collagenous, non-collagenous, background. Following the collagenous region segmentation, non-collagenous regions and background were separately segmented by using binary masking.

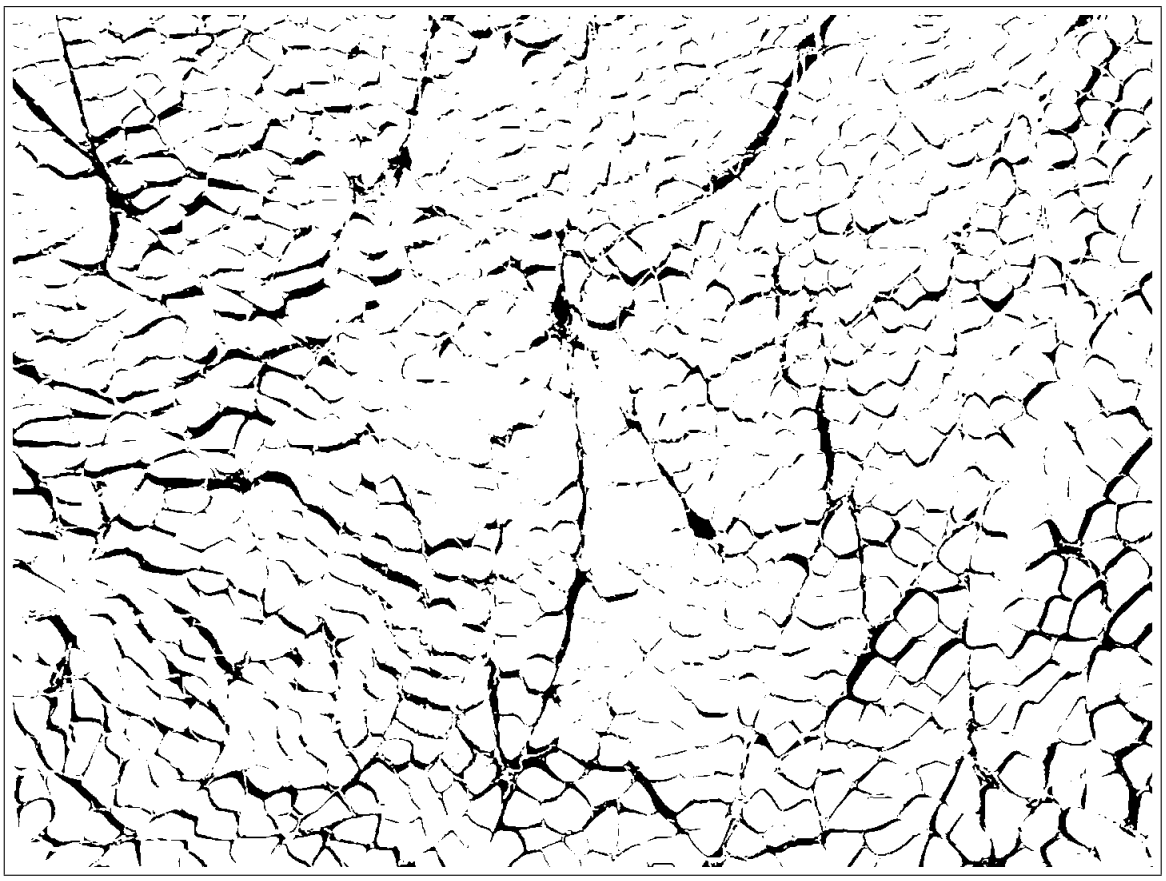

Figure 2.4 Sample histological section of tibialis anterior stained using Gomori trichrome processed by user specific code to differentiate background. Muscle fibers' pixels and collagenous structures' pixels get masked by white color where background's pixels get masked by black color. White mask concludes of muscle fibers and collagenous structures to be analyzed and black mask gets excluded from analysis.

Otsu's thresholding [31] was used to separate background from non-collagenous foregrounds after the collagenous regions were excluded. Acquired domains of these 3 regions were individually identified with exclusive quantities as an indicator of number of pixels at each domain. Collagen ratios of images of muscle tissue sections were calculated by using the following equation:

$$\frac{\textit{Number of pixels at collagenous regions}}{\textit{Number of pixels at collagenous regions} + \textit{non-collagenous regions}} \tag{2.3}$$

All computations were performed using MATLAB release R2015a (The MathWorks Inc., Natick, MA).

2.12 Statistical Analysis

Kruskal-Wallis test was used to test for the effects of BTX-A administration on L_{range}. Two-way ANOVA for repeated measures (factors Δl_{ma} and animal group) was performed separately for the forces of each muscle. Differences were considered significant at $P < .05$. If significant main effects were found, Bonferroni post hoc tests were performed to further locate significant force differences within the factors [32]. For histological assessment, quantitative data gathered via custom-made image processing code and given as numeric values between 0 and 1 depending on pixel amounts. Anderson-Darling Test, Kolmogorov-Smirnov (K-S) Test and Lilliefors Test are used to check the normality of data and results were more often than not consequent as distribution being non-normal. The present study includes two experimental groups, BTX-A, and control. A suitable nonparametric statistical method for histological assessment is The Wilcoxon Rank-Sum Test since the two samples are independent and ordinal. Every muscle group have been subjected to The Wilcoxon Rank-Sum with its own statistical analysis group meaning that EDL muscles of control and BTX-A groups were compared with each other, while TA, SOL, GM and GL were grouped up with their own kinds as well. Differences were considered significant at $P < 0.05$.

3. RESULTS

3.1 Effects of BTX-A on Muscle's Forces

3.1.1 Condition I: GM+GL Lengthening

Active forces

ANOVA (factors: $\Delta l_{ma\_GM\text{-}GL}$ and animal group) showed significant main effects of both factors on GM-GL active forces (e.g., for control group, 18.70 N at $\Delta l_{ma\_GM\text{-}GL}$ = 0 mm) and a significant interaction. Post hoc testing showed significant effects of BTX-A ($\Delta l_{ma\_GM\text{-}GL} < -8$ mm). GM-GL active force reductions equaled e.g., 83.6%, 82.5% and 79.4%, respectively at $\Delta l_{ma\_GM\text{-}GL} = -7$, 0 and 2 mm (3.1) and a total of 79.4%. $L_{range\_GM\text{-}GL}$ decreased significantly (13.2 ± 1.6 mm to 10.0 ± 1.8 mm) (P = 0.02).

Passive forces

ANOVA (factors: $\Delta l_{ma\_GM\text{-}GL}$ and animal group) showed significant main effects of both factors on GM-GL passive forces (e.g., for control group, 0.50 N at $\Delta l_{ma\_GM\text{-}GL}$ = 2 mm), but no significant interaction (Figure 3.1). Passive forces of the BTX-A group were on average 16.3% higher than those of the control group. Although a mean value of 0.17 N for control group with a mean value of 0.19 N for BTX-A group is not sufficient enough to conclude a significant change.

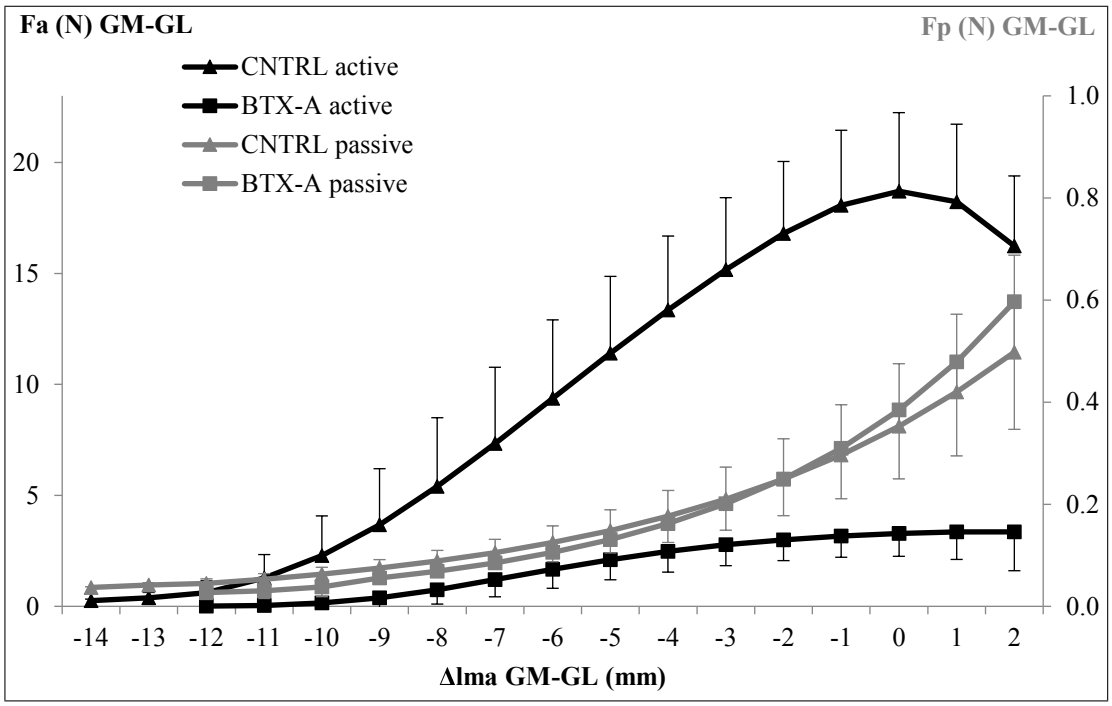

Figure 3.1 Forces of the GM-GL muscles as function of increasing GM-GL muscle length. Active as well as passive isometric forces are shown as mean values ± SD for the control and BTX-A groups. Forces obtained after GM-GL muscle-tendon complex lengths were altered exclusively. GM-GL muscle-tendon complex length is expressed as a deviation from its optimum length $\Delta l_{ma\_GM\text{-}GL}$ (mm). Figure shows a representation of the significant decrease found for muscles' length range of active force exertion after BTX-A injection. For the control group $L_{range\ control} = 13.2 \pm 1.6$ mm, whereas for the BTX-A group $L_{range\ BTX\text{-}A} = 10.0 \pm 1.8$ mm.

3.1.2 Condition II: GM+GL+SOL Lengthening

Active forces

ANOVA (factors: $\Delta l_{ma\_GM\text{-}GL}$ and animal group) showed significant main effects of both factors on SOL active forces (e.g., for control group, 1.64 N at $\Delta l_{ma\_GM\text{-}GL} = 0$ mm), but no significant interaction. BTX-A caused on average 24% force drop (Figure 3.2). L_{range_SOL} decreased significantly (11.4 ± 1.1 mm to 8.5 ± 1.4 mm) ($P = 0.0026$)

Passive forces

ANOVA (factors: $\Delta l_{ma\_GM\text{-}GL}$ and animal group) showed significant main effects of both factors on SOL passive forces, but no significant interaction (Figure 3.2).

Passive forces of the BTX-A group (e.g., 0.8 N at $\Delta l_{ma\_GM\text{-}GL} = 2$ mm) were on average 128.8% higher than that of the control group.

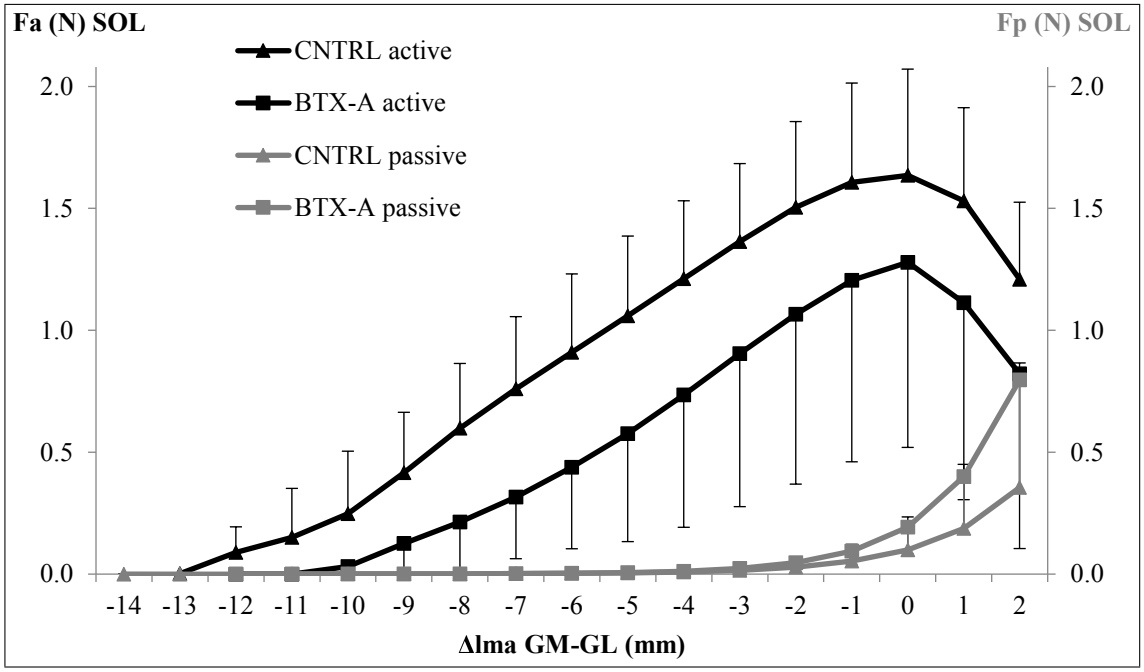

Figure 3.2 Forces of the SOL muscle as a function of increasing GM-GL muscle length. Active as well as passive isometric forces are shown as mean values ± SD for the control and BTX-A groups. Forces obtained after GM-GL and SOL muscle-tendon complex lengths were altered together. GM-GL muscle-tendon complex length is expressed as a deviation from its optimum length $\Delta l_{ma\_GM\text{-}GL}$ (mm). Figure shows a representation of the significant decrease found for muscles' length range of active force exertion after BTX-A injection. For the control group $L_{range\ control} = 11.4 \pm 1.1$ mm, whereas for the BTX-A group $L_{range\ BTX\text{-}A} = 8.5 \pm 1.4$ mm.

3.1.3 Condition III: TA Lenghtening

Active forces

ANOVA (factors: Δl_{ma_TA} and animal group) showed significant main effects of both factors (animal group $P = 0.04$, and Δl_{ma_TA} $P = 0.0007$) on TA active forces, but no significant interaction. On average, TA active forces decreased by 20.7 ± 15.4 % (Figure 3.3). The decrease in L_{range_TA} (10.2 ± 1.3 mm to 9.2 ± 1.5 mm) was not significant ($P = 0.17$).

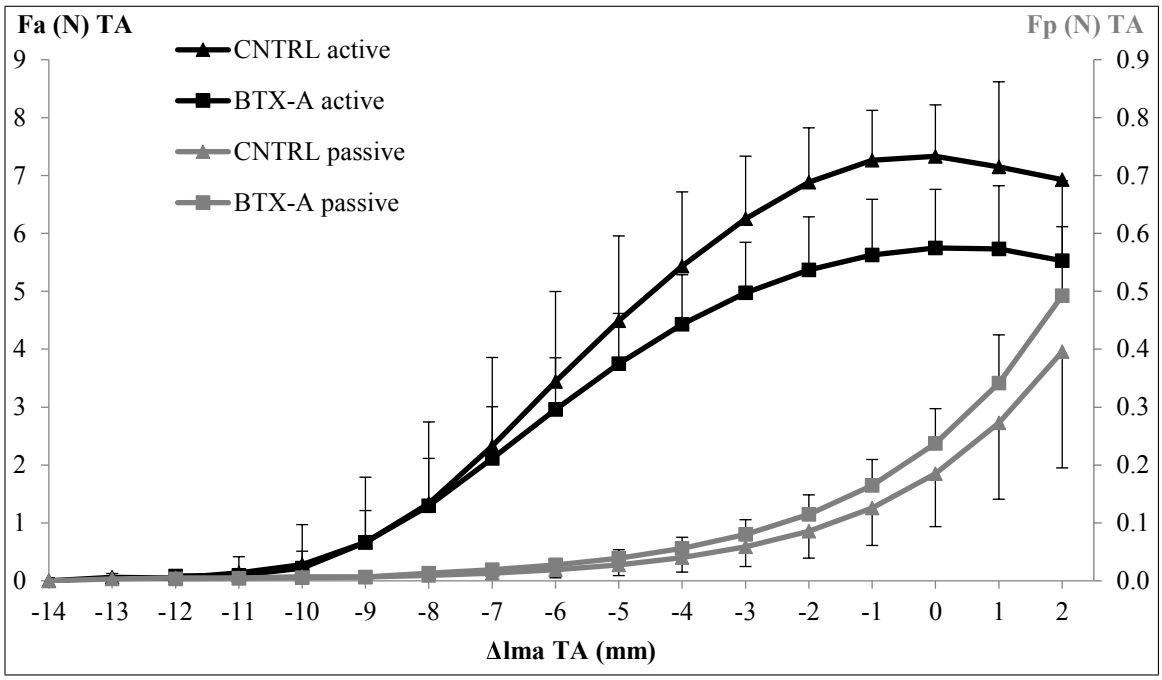

Figure 3.3 Forces of the TA muscle as a function of increasing TA muscle length. Active as well as passive isometric muscle forces are shown as mean values ± SD for the control and BTX-A groups. Forces obtained after TA muscle-tendon complex lengths were altered exclusively. TA muscle-tendon complex length is expressed as a deviation from its optimum length Δl_{ma_TA} (mm).

Passive forces

ANOVA (factors: Δl_{ma_TA} and animal group) showed significant main effects of both factors on TA passive forces, as well as a significant interaction (Figure 3.3). Post hoc test located significant effects of BTX-A at longer TA lengths ($\Delta l_{ma\_TA} < 0$ mm) causing TA passive forces to increase (maximally by 25.0%).

3.1.4 Condition IV: Relative Position — distal forces of EDL muscle at EDL Optimum Length

ANOVA (factors: $\Delta l_{EDL\ position}$ and animal group) showed significant main effects of both factors on EDL distal active forces (Figure 3.4), and a significant interaction. Post-hoc test indicated significant major effects of BTX-A injection for all positions tested except $\Delta l_{EDL\ position} = 5$ mm. The average force difference between

EDL distal active forces of control and BTX groups was 22.78%.

For the control group, the EDL distal force measured at -5 mm (2.02 ± 0.31 N) decreased by 39.07% with altered $\Delta l_{\text{EDL position}}$ (to 1.23 N $\pm$ 0.62 at 5 mm). In the BTX group, EDL distal force measured at -5 mm (1.60 ± 0.95 N) decreased by 40.75% with altered $\Delta l_{\text{EDL position}}$ (to 0.95 N $\pm$ 0.19 at 5 mm).

ANOVA showed significant main effect of only $\Delta l_{\text{EDL position}}$ on EDL distal passive forces (Figure 3.4).

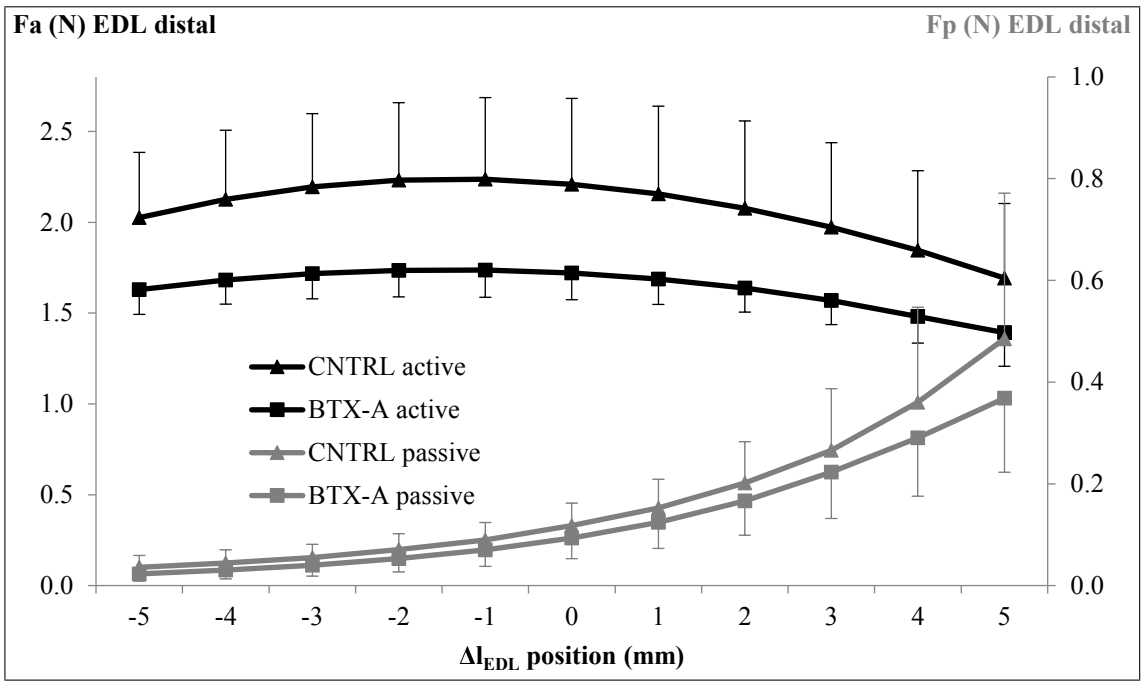

Figure 3.4 Forces of the EDL muscle as a function of changing EDL relative muscle position. Active as well as passive isometric muscle forces are shown as mean value $\pm$ SD for the control and BTX-A groups. EDL distal forces obtained in the high length condition. EDL muscle-tendon complex length is expressed as a deviation from its optimum length.

3.1.5 Condition V: Relative Position — proximal forces of EDL muscle at EDL Optimum Length

ANOVA (factors: $\Delta l_{\text{EDL position}}$ position and animal group) showed significant main effects of both factors on EDL proximal active forces (Figure 3.5), but no significant interaction. On average the force difference between EDL proximal active forces of control and BTX groups was 43.77%.

For the control group, the EDL proximal force measured at -5 mm (2.56 ± 0.24 N) decreased by 72.46% with altered $\Delta l_{\text{EDL position}}$ (to 0.71 N $\pm$ 0.47 at 5 mm). In the BTX group, EDL proximal force measured at -5 mm (2.04 ± 0.17 N) decreased by 93.85% with altered $\Delta l_{\text{EDL position}}$ (to 0.13 ± 0.09 N at 5 mm).

ANOVA showed significant main effect of only $\Delta l_{\text{EDL position}}$ on EDL proximal passive forces (Figure 3.5).

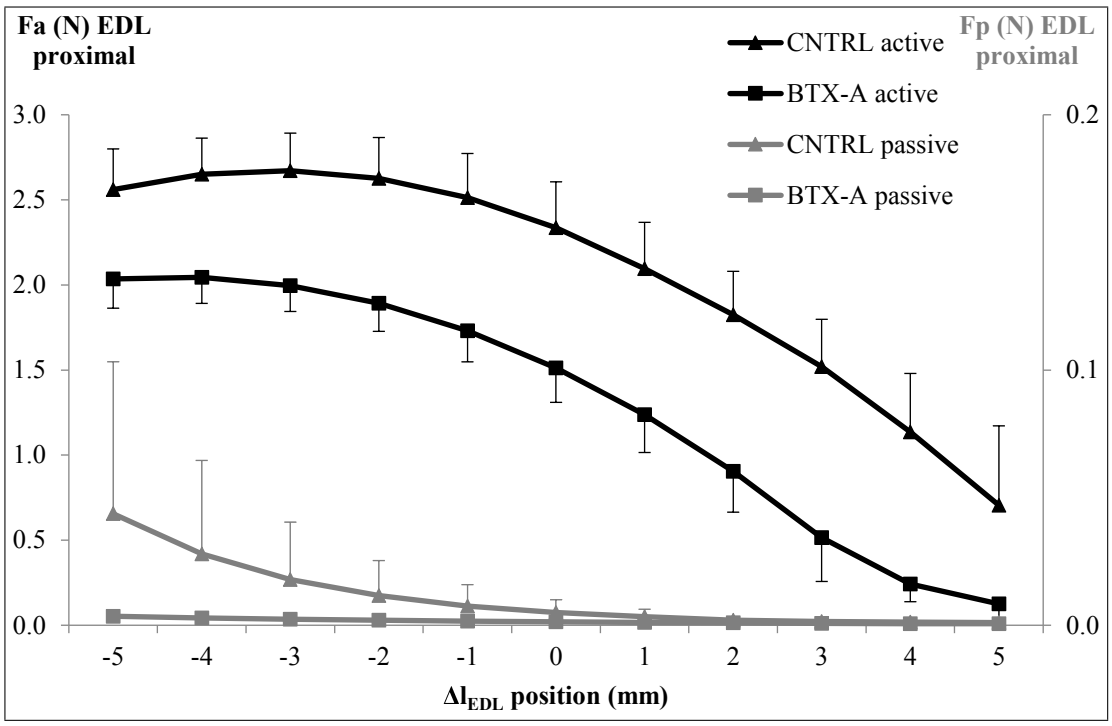

Figure 3.5 Forces of the EDL muscle as a function of changing EDL relative muscle position. Active as well as passive isometric muscle forces are shown as mean value $\pm$ SD for the control and BTX-A groups. EDL proximal forces obtained in the high length condition. EDL muscle-tendon complex length is expressed as a deviation from its optimum length.

3.2 Effects of BTX-A on Proximo-distal Active Force Differences

ANOVA (factors: $\Delta\text{posit}_{\text{EDL}}$ and animal group) showed significant main effects of both factors on EDL proximo-distal ($F_{\text{distal}} - F_{\text{proximal}}$) active force differences (Figure 3.6). For the control group, the force difference values were as high as -0.55 ± 0.34 N at $\Delta\text{posit}_{\text{EDL}} = -4$ mm and 0.53 ± 0.97 N at $\Delta\text{posit}_{\text{EDL}} = 5$ mm. After BTX-A injection, these values changed to -0.35 ± 0.11 N at $\Delta\text{posit}_{\text{EDL}} = -4$ mm and 0.61 ± 0.51 N at $\Delta\text{posit}_{\text{EDL}} = 5$ mm.

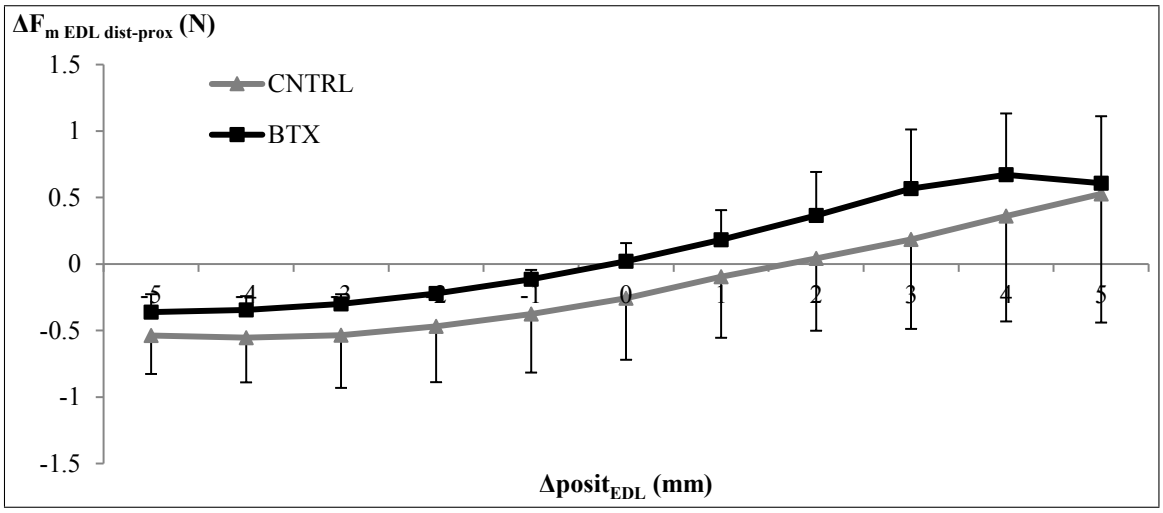

Figure 3.6 EDL proximodistal active force differences as a function of changing EDL relative muscle position. Force differences, calculated as $F_{\text{distal}} - F_{\text{proximal}}$ for the control group and the BTX-A injected group of animals, are presented as mean value ± SD. The EDL muscle-tendon complex relative position changes ($\Delta\text{posit}_{\text{EDL}}$) are expressed as deviation from the proximal end position ($\Delta\text{posit}_{\text{EDL}} = -5$ mm) to the distal end position ($\Delta\text{posit}_{\text{EDL}} = 5$ mm). A positive force difference indicates that a net epimuscular myofascial load is exerted on the EDL in the proximal direction, and a negative force difference indicates a distally directed net epimuscular myofascial load.

3.3 Effects of BTX-A on Intramuscular Collagenous Tissue Content

3.3.1 Gastrocnemius Lateralis (GL)

The percentage of intramuscular connective tissue content values for GL muscle of the BTX- A group (mean ± SD = 20.4% ± 2.7%, respectively) was significantly higher than that for GL muscle of the control group (mean ± SD = 13.6% ± 4.1%, respectively) ($P < 0.001$). BTX-A caused a significant increase in collagen content for GL by 50.3%.

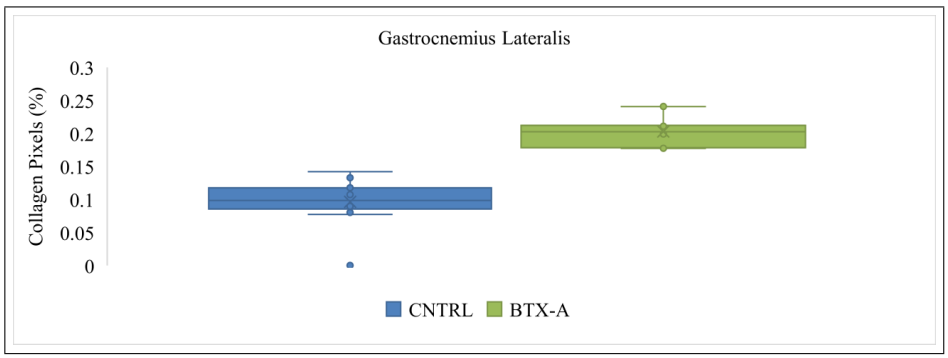

Figure 3.7 Collagen content as in pixel ratio of intramuscular connective tissue to muscle fibers. 5 μm cross-sections were cut for every 20 μm at the mid-portions of GL muscles for both control and BTX-A groups. The sections were stained using Gomori trichrome and the stained sections were photographed with 10x magnification under the microscope. Identical locations at tissue placements were analyzed for both control and BTX-A groups.

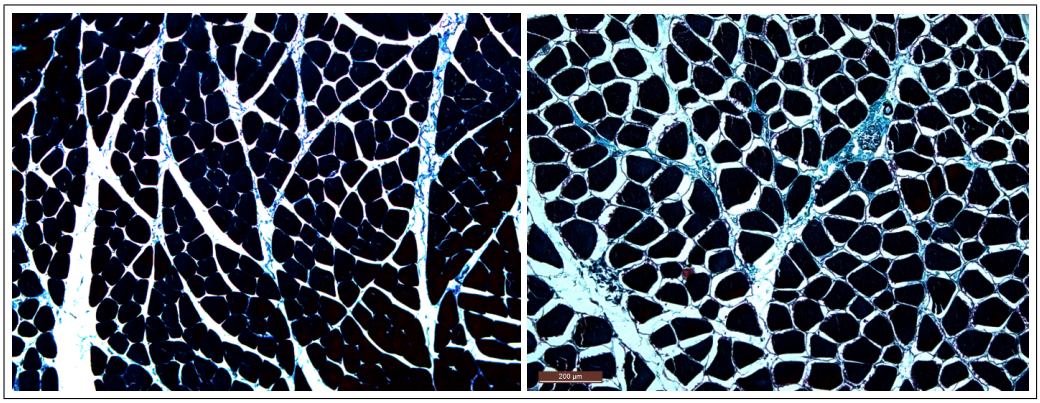

Figure 3.8 Sample histological sections of gastrocnemius lateralis stained using Gomori trichrome. The sections exemplify intramuscular tissue content for Control (left) and BTX-A (right) groups (with 20x magnifications for demonstration purposes). Gomori trichrome stain gives a light (green to blue) color to the connective tissues. The whole cross-sectional area of the images taken with 10x magnifications were analyzed.

3.3.2 Gastrocnemius Medialis (GM)

The percentage of intramuscular connective tissue content values for GM muscle of the BTX-A group (mean ± SD = 20.8% ± 5.1%, respectively) was significantly higher than that for GM muscle of the control group (mean ± SD = 15.8% ± 5.6%, respectively) ($P < 0.001$). BTX- A caused a significant increase in collagen content for GM by 31.7%.

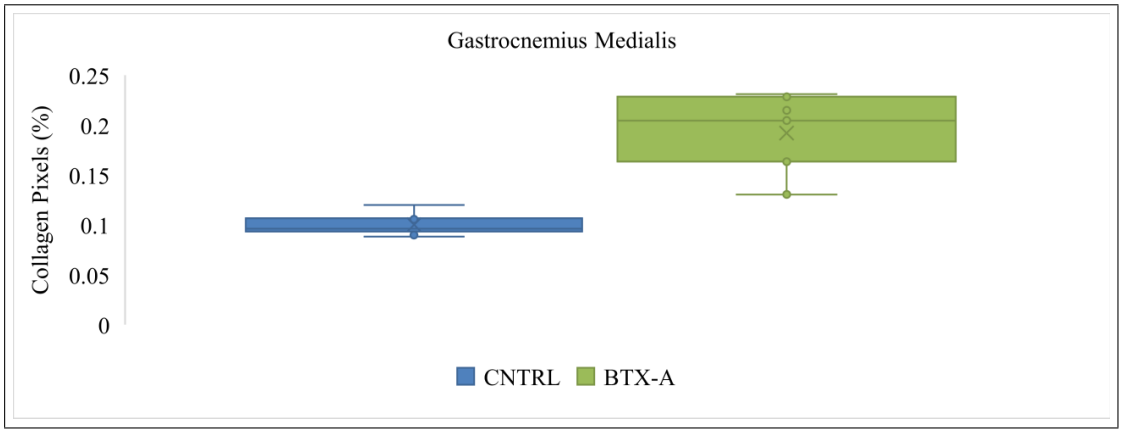

Figure 3.9 Collagen content as in pixel ratio of intramuscular connective tissue to muscle fibers. 5 μm cross- sections were cut for every 20 μm at the mid-portions of GM muscles for both control and BTX-A groups. The sections were stained using Gomori trichrome and the stained sections were photographed with 10x magnification under the microscope. Identical locations at tissue placements were analyzed for both control and BTX-A groups.

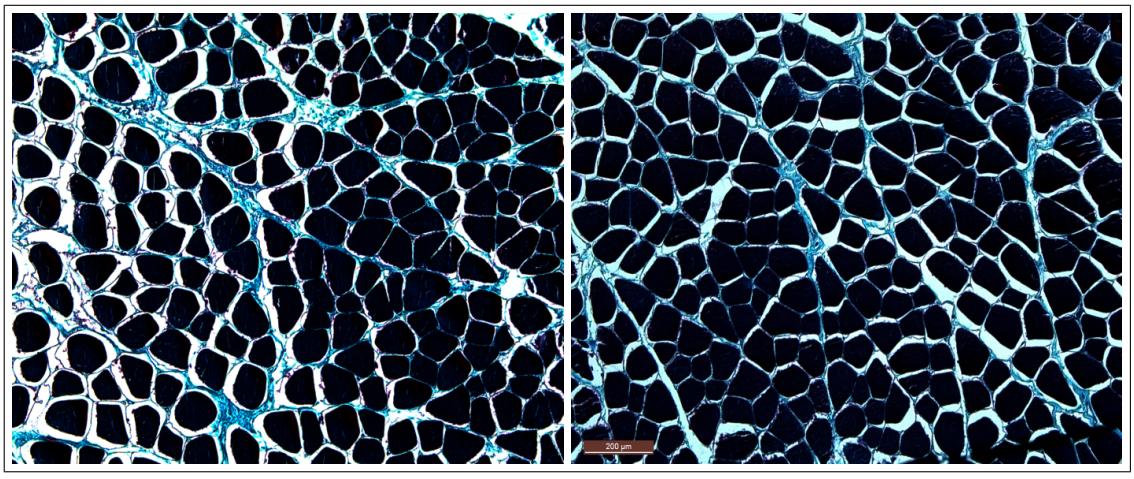

Figure 3.10 Sample histological sections of gastrocnemius medialis stained using Gomori trichrome. The sections exemplify intramuscular tissue content for Control (left) and BTX-A (right) groups (with 20x magnifications for demonstration purposes). Gomori trichrome stain gives a light (green to blue) color to the connective tissues. The whole cross-sectional area of the images taken with 10x magnifications were analyzed.

3.3.3 Soleus (SOL)

The percentage of intramuscular connective tissue content values for SOL muscle of the BTX-A group (mean ± SD = 20.3% ± 5.2%, respectively) was significantly higher than that for SOL muscle of the control group (mean ± SD = 18.2% ± 4.7%, respectively) ($P < 0.001$). BTX-A caused a significant increase in collagen content for SOL by 11.3%.

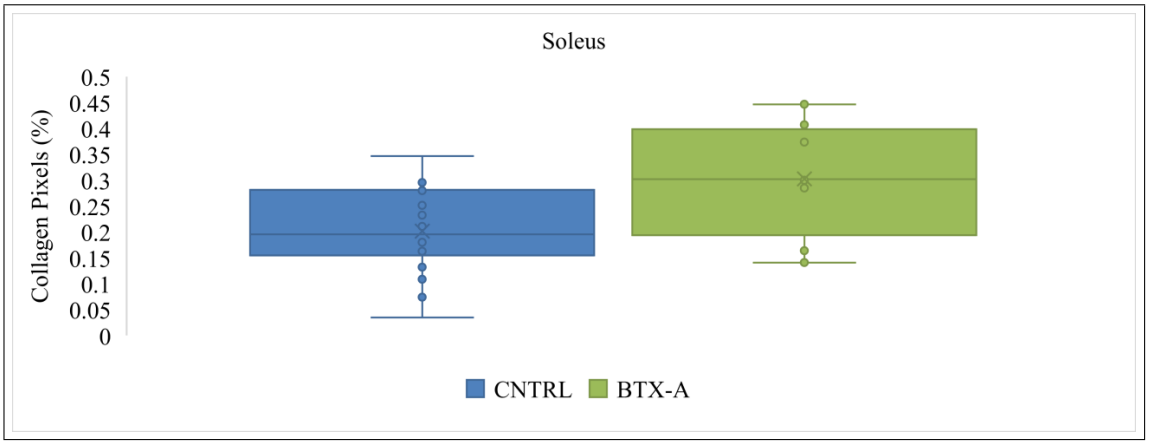

Figure 3.11 Collagen content as in pixel ratio of intramuscular connective tissue to muscle fibers. 5 μm cross-sections were cut for every 20 μm at the mid-portions of SOL muscles for both control and BTX-A groups. The sections were stained using Gomori trichrome and the stained sections were photographed with 10x magnification under the microscope. Identical locations at tissue placements were analyzed for both control and BTX-A groups.

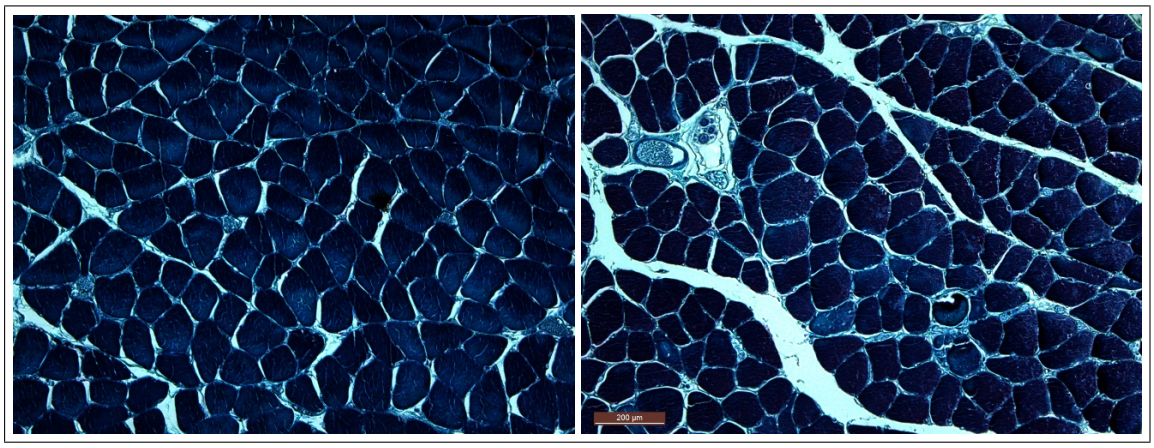

Figure 3.12 Sample histological sections of Gomori trichrome stained soleus muscles. The sections exemplify intramuscular tissue content for Control (left) and BTX-A (right) groups (with 20x magnifications for demonstration purposes). Gomori trichrome stain gives a light (green to blue) color to the connective tissues. The whole cross-sectional area of the images taken with 10x magnifications were analyzed.

3.3.4 Tibialis Anterior (TA)

The percentage of intramuscular connective tissue content values for TA muscle of the BTX-A group (mean ± SD = 19.9% ± 4.9%, respectively) was significantly higher than that for TA muscle of the control group (mean ± SD = 13.8% ± 5.3%, respectively) ($P < 0.001$). BTX-A caused a significant increase in collagen content for TA by 43.7%.

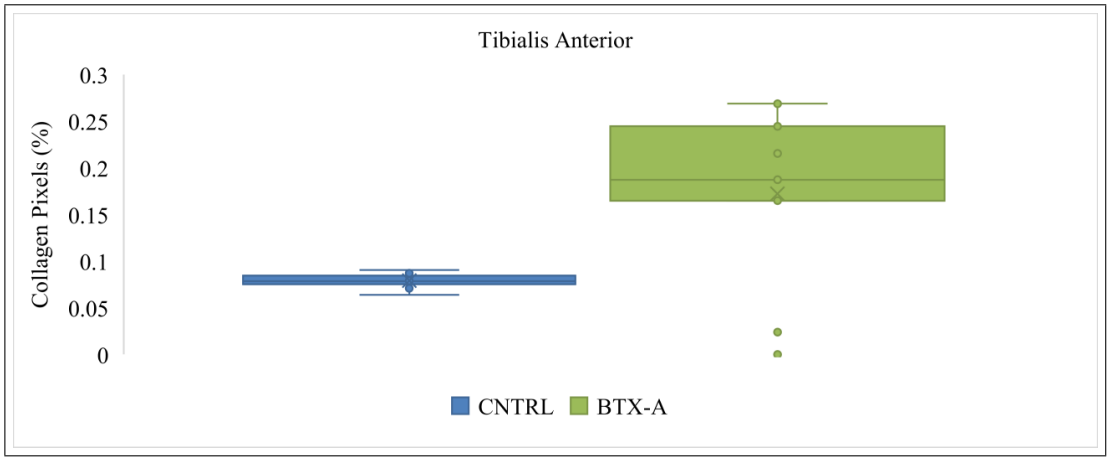

Figure 3.13 Collagen content as in pixel ratio of intramuscular connective tissue to muscle fibers. 5 μm cross-sections were cut for every 20 μm at the mid-portions of TA muscles for both control and BTX-A groups. The sections were stained using Gomori trichrome and the stained sections were photographed with 10x magnification under the microscope. Identical locations at tissue placements were analyzed for both control and BTX-A groups.

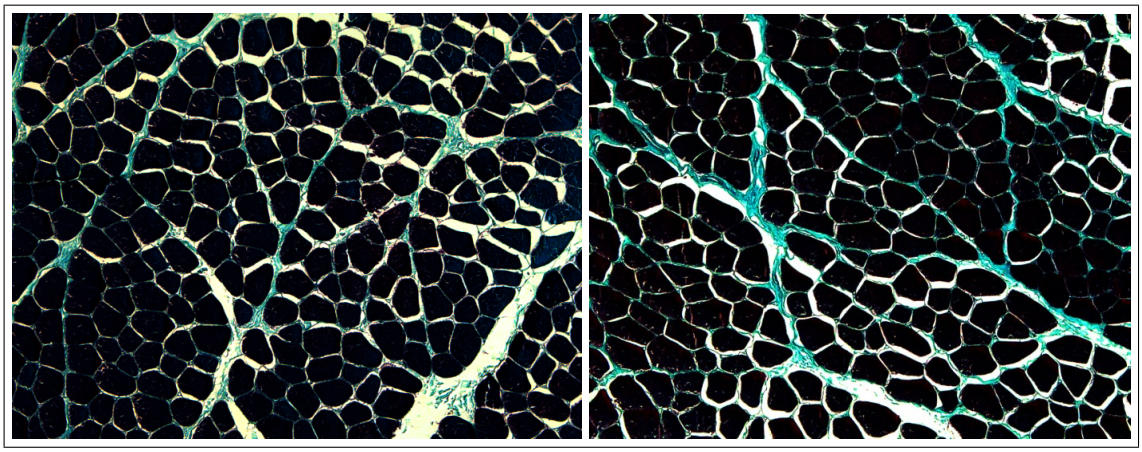

Figure 3.14 Sample histological sections of tibialis anterior stained using Gomori trichrome. The sections exemplify intramuscular tissue content for Control (left) and BTX-A (right) groups (with 20x magnifications for demonstration purposes). Gomori trichrome stain gives a light (green to blue) color to the connective tissues. The whole cross-sectional area of the images taken with 10x magnifications were analyzed.

3.3.5 Extensor Digitorum Longus (EDL)

The percentage of intramuscular connective tissue content values for EDL muscle of the BTX-A group (mean ± SD = 19.2% ± 4.0%, respectively) was significantly higher than that for TA muscle of the control group (mean ± SD = 14.9% ± 4.0%, respectively) ($P < 0.001$). BTX-A caused a significant increase in collagen content for EDL by 28.7%.

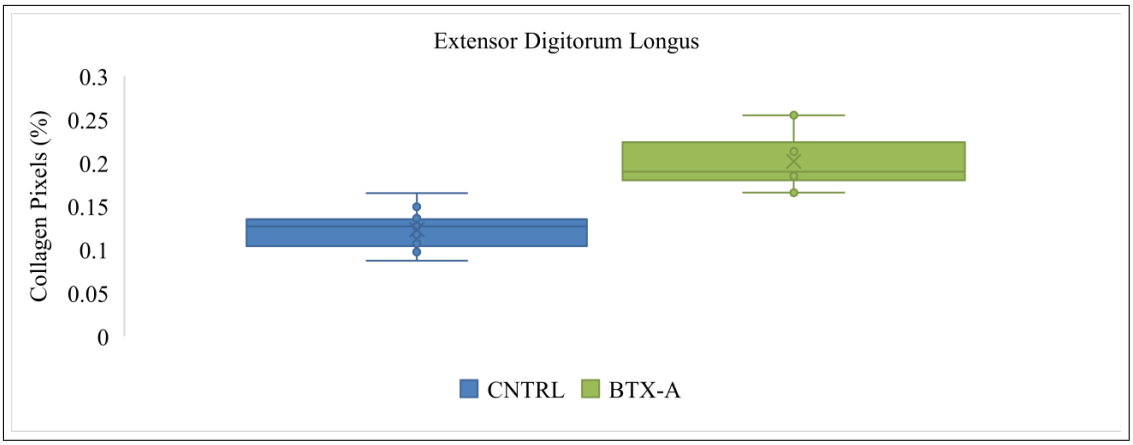

Figure 3.15 Collagen content as in pixel ratio of intramuscular connective tissue to muscle fibers. 5 μm cross-sections were cut for every 20 μm at the mid-portions of EDL muscles for both control and BTX-A groups. The sections were stained using Gomori trichrome and the stained sections were photographed with 10x magnification under the microscope. Identical locations at tissue placements were analyzed for both control and BTX-A groups.

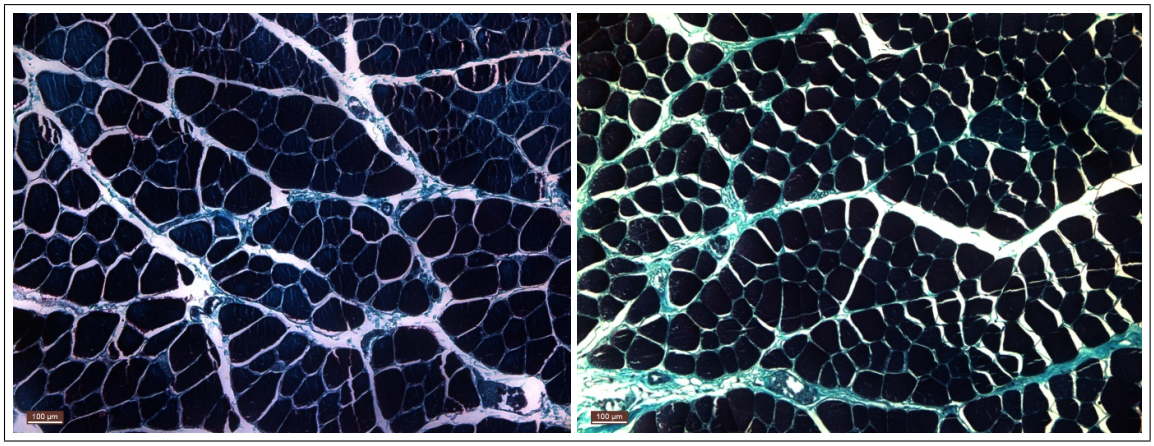

Figure 3.16 Sample histological sections of extensor digitorum longus stained using Gomori trichrome. The sections exemplify intramuscular tissue content for Control (left) and BTX-A (right) groups (with 20x magnifications for demonstration purposes). Gomori trichrome stain gives a light (green to blue) color to the connective tissues. The whole cross-sectional area of the images taken with 10x magnifications were analyzed.

4. DISCUSSION

BTX-A effects on the mechanics of non-injected antagonistic muscles are unknown. The aim of this study was to test some of the possible effects on it meanwhile understanding if those effects would be aligned with injected muscles and non- injected agonistic muscles. Confirming the hypotheses, the present results show that BTX-A injected into GM and GL (1) decreases active forces of the antagonistic TA and EDL; (2) reduces length range of force exertion; (3) increases passive forces of TA and EDL; and (4) increases intramuscular connective tissue content.

The results showed a major indication that diffusion of BTX-A to muscles beyond the injection site is a constant finding. Diffusion of BTX-A via muscle fascia was shown [14]. Spread of BTX-A to adjacent muscle [17] and synergistic muscles of an entire compartment [15],[18],[33] were also shown in animal studies. However, this study is the first to show mechanical effects of BTX-A in antagonistic muscles of an injected muscle.

Methodology and techniques of this particular study do not distinguish the possible mechanisms for spread of toxin to non-injected muscles but plausible mechanisms were shown by previous studies such as diffusion through fascia [14],[34],[35]; flow through bloodstream [36] and spread via axonal pathways [37],[38],[39]. Nonetheless, spread through neuronal transport has been reported under high dosage applications [40],[41]. Even though it requires further experimentation, we would like to emphasize on diffusion through fascia to be a more likely mechanism in our study. It is known that exposure to BTX-A causes muscle atrophy [36],[42],[43]. Injection procedure of our study partially paralyzes subjects' muscles, allowing them to produce force upon electrical stimulation, and causes active force reductions most likely due to muscle atrophy. Therefore, subjects were physically active enough to tend to their needs such as reaching to food and water sources and engage in routine activities as in terms of motion mechanics despite the fact that we did not use cages specifically designed for

promoting activity [44],[45].

Active force reduction at condition I was on average at 79% i.e., 83.6%, 82.5% and 79.4%, respectively at $\Delta l_{ma\_GM\text{-}GL} = -7$, 0 and 2 mm since it was the originally injected muscle, the effect of decrease at force was more pronounced compared to remaining synergistic and antagonistic muscles. Additional to force reduction, we found a significant decrease at range of force exertion, significant increase at passive forces, and a significant increase at intramuscular connective tissue density at these directly injected GM and GL muscles. Altogether, our findings regarding GM and GL muscles as directly injected muscles are as expected from this rat model. At condition II, active force reduction was on average at 24% at agonistic muscle, SOL, and still a profound effect of toxin exposure without being directly injected with it. Our findings at SOL muscle, additional to force reduction, share similar features with GM-GL in the same compartment showing increase at passive forces, narrowing at range of motion and an increase at collagenous structures. These findings so far, indicate that BTX-A affects muscles within the same compartment in an analogue way, whether the exposure takes place through injection or spread, and in line with previous findings where directly injected muscle TA and its synergistic EDL and extensor hallucis longus (EHL) muscles had decreases at their active forces [15],[16],[18] and increases at passive forces of TA [18] and its synergistic muscles EDL and EHL [15],[16]. At condition III, active forces decreased by 13.7% at antagonistic muscle, TA, which was fairly significant for a non-injected muscle to have effects of toxin exposure through leakage and yet still a plausible amount of it. At condition IV, distal active forces difference between control and experiment groups was 21.2% whereas at condition V, proximal active forces difference between those groups was 37.1%. Hence, we confirm our hypothesis (1) and conclude that BTX-A injections has effects on forces of non-injected antagonistic muscles, and this shows toxin acting on agonist-antagonist balance beyond the injection site.

Clinical applications of BTX-A injections expected to meet conditions such as an increased L_{range} and reduced passive forces. At condition I, $L_{range\_GM\text{-}GL}$ decreased significantly from $L_{range\ control} = 13.2 \pm 1.6$ mm to $L_{range\ BTX\text{-}A} = 10.0 \pm 1.8$ mm ; at condition II, $L_{range\_GM\text{-}GL}$ decreased significantly from $L_{range\ control} = 12.3 \pm 1.8$

mm to $L_{range\ BTX\text{-}A} = 9.7 \pm 1.3$ mm and also L_{range_SOL} decreased significantly from $L_{range\ control} = 11.4 \pm 1.1$ mm to $L_{range\ BTX\text{-}A} = 8.5 \pm 1.4$ mm ; at condition III, decrease at L_{range_TA} was not significant ($P = 0.17$) between control, $L_{range\ control} = 10.2 \pm 1.3$ mm, and BTX-A, $L_{range\ BTX\text{-}A} = 9.2 \pm 1.5$ mm, groups. This particular study did not test the entire operational length range of the EDL, but the previous study of our research group [15] did and reported a narrowed length range of force exertion due to leakage of BTX-A into the bi- articular extensor digitorum longus causing reduce at L_{range} both proximally and distally. Present data of this research indicates a reduced L_{range} for GM-GL and SOL, and an unchanged L_{range} for TA in line with an earlier experiment, our group has shown no significant changes to L_{range} of rat TA muscle [18]. Effects of BTX-A on range of active force exertion requires further experimentation. In fact, treatment aim favors for an increase at L_{range}, our findings aligned together indicates that BTX-A does not increase L_{range} but most likely can reduce it or very least does not change it at all. In conclusion, we can't confirm or reject our hypothesis (2) but conclude that BTX-A injections do not necessarily increase range of motion.

Additional to widening range of motion, decreasing muscles passive resistance is also a desired outcome of BTX-A applications at CP patients. However, our data had opposing results in the matter of passive forces. At condition I, passive forces of BTX-A group had higher values than those of control group with an average value of 16.3%; at condition II, experiment group had tremendously higher values of passive forces when compared to those of the control group with an average value of 154,9%; at condition III, BTX-A group had passive forces higher than the control group with an average value of 44,2%; however, at condition IV, passive forces of experiment group actually showed decreased values than control group with an average of 21,2%; and yet, at condition V, passive forces of BTX-A group had stupendous decrease when compared to those of the control group and resulted with an average value of 85,48%. Hence, we neither reject nor accept our hypothesis (3) and conclude that BTX-A increased passive forces of TA but not EDL. However, muscles that have been studied, except EDL, had increase at their passive forces. Elevations at those passive forces and their amplitude can be ascribable to mechanical interactions between those muscles. At condition I, altered lengths of GM-GL only effects passive forces to an extent,

but when altered together with SOL length at condition II, increase at passive forces reach to much more higher magnitudes. Passive forces of SOL drop with a 26% at constant length when only GM-GL lengths are altered but in addition of SOL length alterations, passive forces of SOL rise up with a 154% rate. Whereas, passive forces of GM-GL increase by 16% when SOL kept at constant length, but it decreases by 33% with addition of altered SOL lengths. This fluctuant changes at passive forces of SOL and GM-GL muscles might indicate EMFT effects. Experimental conditions such as fixed knee angle in the reference position can feasibly cause GM-GL belly to displace yielding a proximal relative position difference with SOL. Mutual proximal connections of these muscles being stretched can cause proximally directed loads on SOL and distally directed loads on GM-GL. In condition I, lengthening of the GM-GL yielded also a distal relative position difference with the SOL. Mutual distal connections of these muscles being stretched must have caused proximally directed myofascial loads acting upon GM-GL and that can explain the low increase at passive forces of it. However, in condition II, additional lengthening of SOL eliminates their distal relative position difference. Consequently, altered passive forces indicate the proximal parts of the muscles being affected by myofascial loads acting on, ending up with a decrease at GM-GL and an increase for SOL. At condition III, leakage of BTX-A increases passive forces of TA as foreseen and are consistent with the previous findings, where TA muscle itself was directly injected with toxin [18]. The main difference is that the force drop was higher (by 23%) when injected directly. This suggests that exposure to BTX-A has similar mechanical effects on TA whether the exposure occurs directly through injection or indirectly through leakage. Another finding that suggests these passive force decreases at distally and proximally of EDL muscle being related to EMFT is the increased intramuscular connective tissue content. Increased passive forces suggest more specifically that stiffness of the ECM may have increased. Previously reported elevation of ECM stiffness at isolated rat muscle fiber bundles after BTX-A injection supports this implication [46]. BTX groups having increased intramuscular connective tissue could explain this finding which could be ascribable to the increases at passive forces yet decrease at passive forces of EDL both distally and proximally points to effects of EMFT acting upon them. Previous experimental [18] and model data [47] imply that muscles exposed to BTX-A shows sarcomeres of the muscles shifting to

longer lengths. Paralyzed muscle fibers do not shorten as they would in toxin free muscle on excitation due to the partial paralyzation. As an outcome, the stiffer muscle takes up a lesser portion at the muscle-tendon complex length. Sarcomere shortening in the activated muscle fibers can be restricted because of the interaction of muscle fibers with the ECM. Modeling demonstrates that stiffer ECM increases this effect's influence causing it to have higher importance with increasing muscle length [47]. Existence of such longer sarcomere effect can shorten optimum length of the muscle which might be responsible for the narrowing of L_{range}.

As antagonistic muscles to injected muscle, active force reduction at total was still potent but proximally exerted forces showed a higher value of decrease which might indicate the effect of EMFT acting upon the muscle. Proximo-distal force difference is a shown characteristic of EMFT effect [23] and at longer TA lengths, epimuscular myofascial loads became distally directed for the control group consistently with previous studies [18]. Regardless, for the experiment group, the direction of the net amount of epimuscular myofascial loads did not change, but their amplitude decreased and vanished. BTX-A manipulating inter-synergistic EMFT is directly shown this way and earlier, our research group found the same general effect of diminished inter-synergistic EMFT when BTX-A was injected into the TA [16],[18]. In spite of that, recent findings of this study showed increased TA length just diminished the proximally directed myofascial loads acting on the EDL besides previous reporting showed vanishing EDL proximo-distal force differences for all EDL positions tested [18]. Eventually, active force reductions percentages difference between distal and proximal forces was due to the interaction between BTX-A and EMFT mechanisms and how this interaction affects mechanical loads in inter-antagonistic EMFT. EMFT shows its effects at BTX-A group after the injection but its amplitude changes. This suggests that collagen content of epimuscular connective tissues also increase. Though, this needs to be tested in a new study. However, present experimental conditions yielded no such EMFT in the control group.

A major finding on the effects of BTX-A on intramuscular connective tissue content through collagen density was constant at data, showing significant increases

overall. GM-GL as directly toxin injected muscles had increases at their collagen content by 50.3% and 31.7%, SOL as synergistic muscle had 11.3% increase, TA as antagonistic muscle had 43,7% increase and EDL as antagonistic muscle had 28,7% increase. Hence, we confirm our hypothesis (4) and conclude that BTX-A causes an increase at intramuscular connective tissue not just in the injected muscle and its compartment but also at its antagonistic muscles as well. It is expected to have more pronounced effect when injected with BTX-A directly and GL having the highest increase amount amongst the muscles is aligned with this idea. Increased intramuscular connective tissue content may indicate a stiffer ECM.

One of the limitations at histological staining was the adjustment of protocol according to the sizes of the muscle tissues. GM-GL and TA are much thicker muscles when compared to SOL and EDL in terms of volume. Hence, standardization of the staining has a limitation which can be addressed as either less coloring at thick muscles or over dying at thin muscles - comparison wise- since the volume of the muscles determines the diffusion rate of solvent. Images of tissue slices of thicker muscles had more reliable coloring than those of thinner muscles and their increase at collagen density should be more feasible to how much BTX-A actually causes a change at it. SOL and EDL images had some over-exposure to dye which caused muscle fibers to have a color threshold close to intramuscular connective tissue content. This could result in having more pixels counted as collagen and eventually showing a lesser increase at collagen density.

Another limitation of histological area of interest was the study field sometimes having ruptures occurred most likely at during tissue sectioning, which eventually masked at image processing and excluded from analysis. This could cause very small differences at histological area size being studied amongst different slides.

BTX-A effects on healthy and spastic muscles requires further investigation on its possible spread mechanisms, effects on skeletal muscle structures and functions, and agonist-antagonist balance. Our findings endorse the safety concerns regarding the administration of BTX-A as a therapeutic tool and such findings have clinical importance. Overall, our data shows strong effects of BTX-A on muscles which contradict the treatment aims of BTX-A administration at clinical practice.

Present study reports findings of short-term (5 days) effects of BTX-A injected muscles and their agonistic muscles, but especially highlights the findings on their antagonistic muscles. Therefore, it pioneers the possible future works based on long-term effects of BTX-A administration on skeletal muscles since clinical use of BTX-A is a periodically repeated treatment and its effects on skeletal muscles at long-term require further detailed investigation.

4.1 List of publications produced from the thesis

1. Botulinum Toxin Type-A Has Unknown Complex Effects on Exposed Muscles That Contradict Treatment Aims, C. Kaya, O. Akcan, F. Ateş, C. Yucesoy (2017), *25th Annual Meeting of the European Orthopaedic Research Society (EORS)*, September 2017.

REFERENCES

1. Daniel et al., *Dorland's Illustrated Medical Dictionary*, p. 321. Philadelphia, PA, Saunders/Elsevier, 32nd ed., 2012.

2. Lieber, R. L., *Skeletal Muscle Structure, Function & Plasticity: The Physiological Basis of Rehabilitation*, Lippincott Williams & Wilkins, 2nd ed., 2002.

3. Daniel et al., *Dorland's Illustrated Medical Dictionary*, p. 697. Philadelphia, PA, Saunders/Elsevier, 32nd ed., 2012.

4. Light, N., and A. E. Champion, "Characterization of muscle epimysium, perimysium and endomysium collagens," *The Biochemical Journal*, Vol. 3, no. 219, pp. 1017–1026, 1984.

5. Huijing, P. A., and G. C. Baan, "Myofascial force transmission causes interaction between adjacent muscles and connective tissue: effects of blunt dissection and compartmental fasciotomy on length force characteristics of rat extensor digitorum longus muscle," *Archives of Physiology and Biochemistry*, Vol. 2, no. 109, pp. 97–109, 2001.

6. Rijkelijkhuizen et al., "Extramuscular myofascial force transmission for in situ rat medial gastrocnemius and plantaris muscles in progressive stages of dissection," *The Journal of Experimental Biology*, Vol. 1, no. 208, pp. 129–140, 2005.

7. Rijkelijkhuizen et al., "Extramuscular myofascial force transmission for in situ rat medial gastrocnemius and plantaris muscles in progressive stages of dissection," *The Journal of Experimental Biology*, Vol. 208, pp. 129–140, 2009.

8. Maas et al., "Intermuscular interaction between synergists in rat originates from both intermuscular and extramuscular myofascial force transmission," *Cells Tissues Organs*, Vol. 1, no. 181, pp. 38–50, 2005.

9. Huijing, P. A., "Epimuscular myofascial force transmission between antagonistic and synergistic muscles can explain movement limitation in spastic paresis," *Journal of Electromyography and Kinesiology*, Vol. 17, pp. 708–724, 2007.

10. Huijing et al., "Extramuscular myofascial force transmission also occurs between synergistic muscles and antagonistic muscles," *Journal of Electromyography and Kinesiology*, Vol. 17, pp. 680–689, 2007.

11. Meijer et al., "Myofascial force transmission between antagonistic rat lower limb muscles: effects of single muscle or muscle group lengthening," *Journal of Electromyography and Kinesiology*, Vol. 17, pp. 698–707, 2007.

12. Rijkelijkhuizen et al., "Myofascial force transmission also occurs between antagonistic muscles located in opposite compartments of the rat hindlimb," *Journal of Electromyography and Kinesiology*, Vol. 17, pp. 690–697, 2007.

13. Sheean, G., "Botulinum toxin treatment of adult spasticity: a benefit-risk assessment," *Drug Safety*, Vol. 1, no. 29, pp. 31–48, 2006.

14. Shaari, C. M., and C. A. Yucesoy, "Quantifying the spread of botulinum toxin through muscle fascia," *The Laryngoscope*, Vol. 9, no. 101, pp. 960–964, 1991.

15. Ateş, F., and C. A. Yucesoy, "Effects of botulinum toxin type a on non-injected biarticular muscle include a narrower length range of force exertion and increased passive force," *Muscle & Nerve*, Vol. 6, no. 49, pp. 866–878, 2014.

16. Yucesoy, C. A., A. N. Turkoğlu, S. Umur, and F. Ateş, "Intact muscle compartment exposed to botulinum toxin type a shows compromised intermuscular mechanical interaction," *Muscle & Nerve*, Vol. 1, no. 51, pp. 106–116, 2015.

17. Yaraskavitch, M., T. Leonard, and W. Herzog, "Botox produces functional weakness in non-injected muscles adjacent to the target muscle," *Journal of Biomechanics*, Vol. 4, no. 41, pp. 897–902, 2008.

18. Yucesoy, C. A., Ö. E. Arıkan, and F. Ateş, "Btx-a administration to the target muscle affects forces of all muscles within an intact compartment and epimuscular myofascial force transmission," *Journal of Biomechanical Engineering*, Vol. 11, no. 134, p. 111002, 2012.

19. Peixinho, C. C., N. S. Martins, L. F. de Oliviera, and J. C. Machado, "Reliability of measurements of rat lateral gastrocnemius architectural parameters obtained from ultrasound biomicroscopic images„," *Plos One*, Vol. 2, no. 9, p. 87691, 2014.

20. Shaari, C. M., and I. Sanders, "Quantifying how location and dose of botulinum toxin injections affect muscle paralysis," *Muscle & Nerve*, Vol. 9, no. 16, pp. 964–969, 1993.

21. Jr, J. V. C., T. V. McCaffrey, W. J. Litchy, and J. L. Knops, "The effect of botulinum toxin type a injection on compound muscle action potential in an in vivo rat model," *The Laryngoscope*, Vol. 2, no. 105, pp. 144–148, 1995.

22. Duchen, L. W., "Changes in motor innervation and cholinesterase localization induced by botulinum toxin in skeletal muscle of the mouse: differences between fast and slow muscles," *Journal of Neurolology, Neurosurgery, and Psychiatry*, Vol. 1, no. 33, pp. 40–54, 1970.

23. Huijing, P. A., and G. C. Baan, "Extramuscular myofascial force transmission within the rat anterior tibial compartment: proximo-distal differences in muscle force," *Acta Physiologica Scandinavica*, Vol. 3, no. 173, pp. 297–311, 2001.

24. Sheehan, D. C., and B. B. Hrapchak, "Theory and practise of histotechnology," 1987.

25. Bancroft, J. D., and M. Gamble, "Theory and practice of histological techniques," 6th ed., 2008.

26. Barka, T., and P. J. Anderson, *Histochemistry; Theory, Practice, and Bibliography, New*, York: Harper & Row, 1963.

27. Lillie, R. D., *Histopathologic Technic and Practical Histochemistry, New*, York: McGraw-Hill, 1965.

28. Baldevbhai, P. J., and R. S. Anand, "Color image segmentation for medical images using l* a* b* color space," *IOSR Journal of Electronics and Communication Engineering*, Vol. 2, no. 1, pp. 24–45, 2012.

29. Ovinis, M., D. Kerr, K. Bouazza-Marouf, and M. Vloeberghs, "Localisation of anatomical soft tissue landmarks of the head in ct images," *International Journal of Medical, Health, Biomedical, Bioengineering and Pharmaceutical Engineering*, Vol. 4, no. 9, pp. 496–502, 2010.

30. Phongsuphap, S., and K. Kamolrat, "Perceptual colour features for natural scene image description and retrieval," in *2015 IEEE International Conference on Systems, Man, and Cybernetics*, Kowloon, China, 2015.

31. Otsu, N., "A threshold selection method from gray-level histograms," *Automatica*, Vol. 11, pp. 285–296, 1975.

32. Neter, J., M. H. Kutner, C. J. Nachtsheim, and W. Wasserman, *Applied Linear Statistical Models*, Burr Ridge, Illinois: Richard D. Irwin, Inc, 4 ed., 1996.

33. Yucesoy, C. A., and F. Ateş, "Btx-a has notable effects contradicting some treatment aims in the rat triceps surae compartment, which are not confined to the muscles injected," *Journal of Biomechanics*, Vol. 66, pp. 78–85, 2018.

34. Borodic, G. E., R. Ferrante, L. B. Pearce, and K. L. Smith, "Histologic assessment of dose-related diffusion and muscle fiber response after therapeutic botulinum a toxin injections," *Movement Disorders*, Vol. 9, no. 1, pp. 31–39, 1994.

35. Borodic, G. E., M. Joseph, L. A. Fay, D. Cozzolino, and R. Ferrante, "Botulinum a toxin for the treatment of spasmodic torticollis: Dysphagia and regional toxin spread,," *Head & Neck*, Vol. 12, no. 5, pp. 392–399, 1990.

36. Ansved, T., T. Odergren, and K. Borg, "Muscle fiber atrophy in leg muscles after botulinum toxin type a treatment of cervical dystonia," *Neurology*, Vol. 5, no. 48, pp. 1440–1442, 1997.

37. Antonucci, F., C. Rossi, L. Gianfranceschi, O. Rossetto, and M. Caleo, "Long-distance retrograde effects of botulinum neurotoxin a," *The Journal of Neuroscience*, Vol. 14, no. 28, pp. 3689–3696, 2008.

38. Deinhardt, K., and G. Schiavo, "Endocytosis and retrograde axonal traffic in motor neurons," in *Biochemical Society Symposia*, 2005.

39. Matak, I., L. Back-Rojecky, B. Filipović, and Z. Lacković, "Behavioral and immunohistochemical evidence for central antinociceptive activity of botulinum toxin a," *Neuroscience*, Vol. 186, pp. 201–207, 2011.

40. Cai, B. B., J. Francis, M. F. Brin, and R. S. Broide, "Botulinum neurotoxin type a-cleaved snap25 is confined to primary motor neurons and localized on the plasma membrane following intramuscular toxin injection," *Neuroscience*, Vol. 352, pp. 155–169, 2017.

41. Koizumi, H., S. Goto, S. Okita, R. Morigaki, N. Akaike, Y. Torii, T. Harakawa, A. Ginnaga, and R. Kaji, "Spinal central effects of peripherally applied botulinum neurotoxin a in comparison between its subtypes a1 and a2,," *Frontiers in Neurology*, Vol. 5, p. 98, 2014.

42. Dodd, S. L., J. Selsby, A. Payne, A. Judge, and C. Dott, "Botulinum neurotoxin type a causes shifts in myosin heavy chain composition in muscle," *Toxicon*, Vol. 2, no. 46, pp. 196–203, 2005.

43. Stone, A. V., J. Ma, M. F. Callahan, B. P. Smith, J. P. Garrett, T. L. Smith, and L. A. Koman, "Dose-and volume dependent-response to intramuscular injection of botulinum neurotoxin-a optimizes muscle force decrement in mice," *Journal of Orthopaedic Research*, Vol. 11, no. 29, pp. 1764–1770, 2011.

44. Velders, M., K. Legerlotz, S. J. Falconer, N. S. Stott, C. D. McMahon, and H. K. Smith, "Effect of botulinum toxin a-induced paralysis and exercise training on mechanosensing and signalling gene expression in juvenile rat gastrocnemius muscle," *Experimental Physiology*, Vol. 12, no. 93, pp. 1273–1283, 2008.

45. Virchenko, O., and P. Aspenberg, "How can one platelet injection after tendon injury lead to a stronger tendon after 4 weeks?: Interplay between early regeneration and mechanical stimulation," *Acta Orthopaedica*, Vol. 7, no. 77, pp. 806–812, 2006.

46. Thacker, B. E., A. Tomiya, J. B. Hulst, K. P. Suzuki, S. N. Brember, R. F. Gastwirt, M. L. Greaser, R. L. Lieber, and S. R. Ward, "Gastwirt rf, greaser ml, lieber rl, ward sr, passive mechanical properties and related proteins change with botulinum neurotoxin a injection of normal skeletal muscle.„," *Journal of Orthopaedic Research*, Vol. 3, no. 30, pp. 497–502, 2012.

47. Turkoglu, A. N., P. A. Huijin, and C. A. Yucesoy, "Mechanical principles of effects of botulinum toxin on muscle length-force characteristics: an assessment by finite element modeling," *Journal of Biomechanics*, Vol. 7, no. 47, pp. 1565–1571, 2014.

48. OpenStax, "Anatomy & physiology," 2016.

49. Trotter, J. A., and P. P. Purslow, "Functional morphology of the endomysium in series fibered muscles.," *Journal of Morphology*, Vol. 2, no. 212, pp. 109–122, 1992.

50. Marieb, E. N., and K. Hoehn, *Human Anatomy & Physiology*, Boston: Pearson, 2012.

51. Mass, H., and T. G. Sandercock, "Force transmission between synergistic skeletal muscles through connective tissue linkages," *Journal of Biomedicine and Biotechnology, vol. Article*, Vol. 575672, no. 2010, p. p., 2010.

52. Ateş, F., and C. A. Yucesoy, "Botulinum toxin type-a affects mechanics of non-injected antagonistic rat muscles," *Journal of the Mechanical Behavior of Biomedical Materials*, Vol. 84, pp. 208–216, 2018.